DIAGENESIS AND CONSTRUCTION OF THE BELEMNITE ROSTRUM

by GUNNAR SÆLEN

ABSTRACT. Diagenetic and morphological studies of transversely sliced rostra of six belemnite species were carried out by means of scanning-electron, cathodoluminescence and blue-light fluorescence microscopy, staining of thin sections, total organic content analysis, as well as x-ray diffractometry. Diagenesis has not destroyed the laminar morphology of rostra in most cases, and diagenetic alterations indicate that the original mineralogy was low-Mg calcite. A revised interpretation of the construction of belemnite rostra is given, where composite radial structures accreting periodically around the surface are suggested as the principal elements. Organic matter is distributed throughout the rostrum, and is probably both inter- and intra-crystalline. Variation in the organic content along radial structures gives rise to a concentric growth pattern. This variation is often subtle, making growth-rings difficult to define. Müller-Stoll's (1936) concept of a rostrum consisting of discrete alternating inorganic and organic layers is thought to be invalid.

THE purpose of this paper is to describe the morphology and diagenetic alterations of selected belemnite rostra. Previous researchers on the subject have applied just one or two techniques, and it is the aim of this paper to show that more varied information can be extracted by using several methods.

BRIEF REVIEW OF THE MORPHOLOGY AND DIAGENESIS OF THE BELEMNITE ROSTRUM

The rostrum (also referred to as orthorostrum or guard) consists of the following elements (text-fig. 1).

The alveolus (text-fig. 1B) is a conical cavity at the anterior part of rostrum where the chambered part of the shell or phragmocone is situated (text-figs. 1A). In some species (e.g. *Belemnellocamax mammillatus mammillatus* (Nilsson) and *Neohibolites minimus* (Miller) studied here), the most anterior rostral layers are frequently corroded to widen the alveolus and create a shallow depression, the pseudoalveolus (Christensen 1975; Spaeth 1971*a*).

The primordial rostrum is the first rostrum-like structure to form at the apex of protoconch (i.e. incipient chamber; text-fig. 1A), believed to be made up of an anterior inorganic (aragonitic) and a posterior organic part (Bandel *et al.* 1984, p. 277). Due to diagenetic alteration, this structure has not been observed in the specimens studied.

Growth-lines, or growth-rings (text-fig. 1B), have traditionally been interpreted as alternating organic and inorganic layers of the rostrum ('laminae obscurae' and 'laminae pellucidae' of Müller-Stoll 1936). This concentric layering is regarded as primary (see Spaeth *et al.* 1971), though the laminae obscurae are considered to have been modified by diagenesis in most cases (Müller-Stoll 1936; Jeletzky 1966; Barskov 1970; Spaeth 1971*a*).

Radial structures (text-fig. 1B) have traditionally been regarded as formed by crystals which traverse the growth-lines more or less perpendicularly. Their coarse crystalline nature is attributed by most researchers to recrystallization (Jeletzky 1966, p. 108; Spaeth 1971*a*, p. 22).

[Palaeontology, Vol. 32, Part 4, 1989, pp. 765–798, pls. 84–87.]

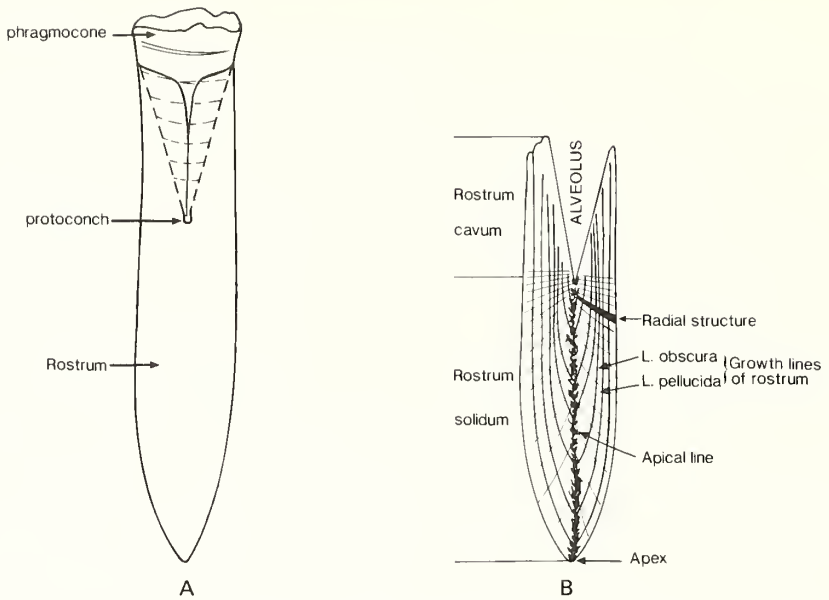

TEXT-FIG. 1. Shell morphology of schematized rostrum. A, rostrum and part of fractured phragmocone situated in the anterior hollow, the alveolus; B, left lateral, longitudinal section through the median plane of a schematized rostrum.

The apical line (text-fig. 1B) is the axis of the rostrum that marks the trajectory of the apex during successive growth stages. The spherulitic nature of the radial structures in this region, combined with diagenetic alteration, frequently give the impression of a discrete morphological feature (Swinnerton 1936–55, p. 14; Sturz-Köwing 1960, p. 61; Spaeth 1971*a*, pp. 24–25). Some authors regard the apical line as an orginally organic feature (Bandel *et al.* 1984, pp. 285, 287).

The apex (text-fig. 1B) usually refers to the most posterior part of the rostrum, but can also refer to the most posterior part of other morphological features (e.g. the phragmocone).

Diagenesis of belemnite rostra has been a much debated subject, especially since Urey *et al.* (1951) based their palaeotemperature curves on $\delta^{18}O$ measurements of this part of the shell. The majority of fossilized rostra consists of low-Mg calcite, though some are reported to be partly aragonitic (Barskov 1970; Spaeth 1971*a*, 1971*b*, 1973; Spaeth *et al.* 1971; H. Mutvei *pers. comm.* 1984). The original mineralogy, however, has been claimed to be:

(1) calcite, advocated by most researchers (see Brand and Morrison 1987, pp. 100–101), based on;
a) the textural and optical regularity of belemnite rostra; (Sandberg 1983, p. 273; Bandel *et al.* 1984),
b) specimens with aragonitic skeletal parts preserved still have calcitic rostra (Sandberg 1983, p. 273), and
c) chemical criteria (Veizer 1974; Brand and Morrison 1987), or
(2) aragonite or partly aragonitic (Spaeth 1971*b*, 1973; Barskov 1970, 1972).

Some palaeontologists claim that the rostrum was originally porous (Spaeth 1971*b*, 1973, 1975; Veizer 1974), while others think of it as originally impervious (Bandel *et al.* 1984, p. 300).

TABLE 1. Material. Cp, *Cylindroteuthis puzosiana*; Hh, *Hibolithes* (*Hibolithes*) *hastatus*; As, *Aulacoteuthis speetonensis*; Ne, *Neohibolites ewaldi*; Nm, *Neohibolites minimus*; Bm, *Belemnellocamax mammillatus mammillatus*; sst. sandstone; bitumin., bituminous; calc., calcite; LBC, London Brick Company

Species	Collected by	No. of specim.	Lithology	Stratigraphic level	Locality	Map reference
Cp	(a) G. Sælen; Bergen University	13	Bitumin. clay	Middle Oxford Clay, Upper Callovian	LBC-pit, Stewartby	TL015413
	(b) Dr H. Powell; Oxford Univ. Museum	19	Bitumin. clay	*K. jason* subzone, Lower Oxford Clay, Middle Callovian	LBC-pit, NNW of Yaxley, near Peterborough	TL176944
	(c) G. Sælen	6	sst. with varying content of calc. and mica	Fensfjord Fm.	North Sea boreholes 31/6–1 and 31/4–5	—
Hh	G. Sælen	1	Bitumin. clay	Upper Callovian	Stewartby	TL015413
		4	Bitumin. clay	*Q. lamberti* zone, Tidmoor Point Clays	Tidmoor Point, Dorset	SY643787
		6	Bitumin. clay	Upper Oxford Clay, Lower Oxfordian	Warboys, ~ 25 km SE of Peterborough	TL306818
As	O. Walderhaug; Rogalandsforskning	1	Black, highly pyritic clay	probably from the LB2 bed, Barremian (Neale 1974)	Speeton Beck, Speeton	TA1551754
Nc	O. Walderhaug	1	Pale, brick-red soft chalk	Red Chalk, Upper Albian, probably the W-division (Neale 1974)	Speeton Beck, Speeton	TA1551754
Nm	G. Sælen	130	Pale grey clay	Gault Clay, probably the *H. spathi* subzone	Double Arches pit	SP939290
					Mundays Hill	SP940280
Bm	Dr W. K. Christensen; Geol. Mus. of Copenhagen	40	Biocalcarenite	Uppermost Lower Campanian	Ignaberga New Quarry	Topogr. maps of Sweden; 3DKristianstadSO VC288195

MATERIAL AND METHODS

Recent investigators have applied special techniques to unravel the original morphology, mineralogy, and degree of diagenetic alteration of belemnite rostra. These methods include scanning-electron microscopy (see Spaeth 1971*b*, 1973; Barskov 1970, 1972; Bandel *et al.* 1984), X-ray diffractometry (see Vetter 1968), stable isotope analysis (see Fritz 1965; Longinelli 1969; Spaeth *et al.* 1971; Stevens and Clayton 1971; Küspert 1982) as well as minor- and trace-element analyses (Veizer 1974; Hückel and Hemleben 1976). Since these methods do not give unequivocal results when applied singly (see Brand and Morrison 1987, p. 88), a multi-method approach has been applied in the present study. The methods used include scanning-electron microscopy (SEM), cathodoluminescence (CL) and blue-light fluorescence (BLF) microscopy, thin-section staining (Dickson 1966), X-ray diffractometry (XRD), and total organic carbon (TOC) analyses. These techniques have been used to study six selected belemnite species from different stratigraphic levels and sedimentary environments (Table 1). Some of the specimens were additionally subjected to stable isotope analyses and minor- and trace-element analyses (Sælen and Karstang 1989).

Scanning-electron microscopy

Cutting and grinding of slabs. When the specimen is cross-sectioned surfaces are produced that are approximately mirror-image equivalents (position 1, text-fig. 2*a*). One of these paired surfaces (numbered 1–5 in text-fig. 2*a*) was then consistently prepared for SEM, and the other for thin-sectioning.

Chemical agents. The application of chemical agents makes the growth-rings visible under SEM, and thus is a powerful tool in unravelling the construction of the rostrum. Several chemicals have been applied, with different aims (Table 2).

a) Acids preferentially etch the carbonate-rich portions. The use of weak acids (e.g. 1% HCl) gives 'surface reaction controlled dissolution' (Berner 1980, p. 106).

b) 35% hydrogen peroxide is a powerful oxidizing medium which readily attacks organic matter and can thus be used to pin-point its distribution in the rostra. This reaction, moreover, produces organic acids which lower the pH and finally ease the dissolution of the carbonate itself. Consequently, areas rich in organic matter will also show the most profound etching effect.

c) Glutardialdehyde, $OHC(CH_2)_3CHO$, is an excellent fixing agent of organic matter, and it is known to react specifically with proteins (Iversen 1973). Moreover, glutardialdehyde easily oxidizes to glutaric acid (Sabatini *et al.* 1964), and a 25% solution (Merck) maintained at a pH of $\sim$ 4·0 has been used to benefit from both the fixing properties of the aldehyde and the etching effect of the acid.

After treatment with one of the chemicals, the slabs were washed gently with water and dried. They were then mounted on SEM stubs and coated with gold-palladium for 2·5 to 9 mins.

Cathodoluminescence (CL)

Primary biogenic carbonate is thought to be non-luminescent (Glover 1977; Czerniakowski *et al.* 1984; Popp *et al.* 1986; Sælen and Karstang 1989), and CL studies can thus provide information as to the diagenetic alteration of rostra. The present study used diamond-polished thin sections (cf. Nickel 1978, p. 79; Dravis and Yurewicz 1985, p. 796) and a Technosyn LTD8200 CL device (gun current $\sim$ 150 μA) coupled with an Ortholux 2 pol-BK microscope.

Blue-light fluorescence (BLF)

BLF studies can give valuable information on primary biogenic as well as diagenetic fabrics. Though the causes of fluorescence in carbonate rocks have not been systematically evaluated, it is known that both organic and inorganic substances can create fluorescence (van Gijzel 1979; Dravis and Yurewicz 1985). A Zeiss photomicroscope III and blue-light filter with wave length of 400–440 ηm (van Gijzel 1979, p. 11; Dravis and Yurewicz 1985, p. 796) were used in the present study.

TABLE 2. Chemicals applied to reveal fabrics under SEM

Medium	Concentration	Reaction time	Effect
Hydrochloric acid	1%	3 to 6 mins	etching
Glutaric acid	100 mg/350 ml	6 mins	etching
Hydrogen peroxide	35%	up to 48 hrs	oxidation/etching
Glutardialdehyde	25%	6 to 11 hrs	fixation/etching

Stained thin sections

After CL and BLF inspection, the thin sections were stained with Alizarin Red-S and K-ferricyanide as described by Dickson (1966).

X-ray diffractometry (XRD)

Fifteen samples of rostrum cavum and rostrum solidum (see text-fig. 1B) of all six belemnite species were analysed by means of a Philips PW 1710 diffractometer, using the laboratory facilities of Norsk Hydro Research Centre, Bergen.

Total organic carbon (TOC) of rostra

Twelve samples from the species *Cylindroteuthis puzosiana*, *Hibolithes* (*H.*) *hastatus*, *Neohibolites minimus* and *Belemnellocamax mammillatus mammillatus* were dissolved in 2N HCl and centrifuged. This procedure was repeated three times to ensure that all inorganic carbonate was dissolved. The insoluble part was then washed 3 to 4 times with purified water and analysed for its TOC by means of a C244HP element analyser (facilities of Norsk Hydro Research Centre, Bergen).

SYSTEMATIC PALAEONTOLOGY

The classification below is based on Rogér (1952), Jeletzky (1966), Spaeth (1971*a*), Christensen (1975), Riegraf (1981) and Mutterlose (1983), and the systematic descriptions are listed in Table 3.

Order BELEMNITIDA Zittel, 1895
Suborder BELEMNITINA Zittel, 1895
Family CYLINDROTEUTHIDAE Stolley, 1919
Genus CYLINDROTEUTHIS Bayle, 1878 (Stolley, 1919)
Species *Cylindroteuthis puzosiana* (d'Orbigny, 1860)
Family BELEMNITIDAE d'Orbigny, 1845
Genus HIBOLITHES Montfort, 1808
Subgenus HIBOLITHES Montfort, 1808
Species *Hibolithes* (*Hibolithes*) *hastatus* Montfort, 1808
Genus NEOHIBOLITES Stolley, 1911
Species *Neohibolites ewaldi* (von Strombeck, 1861)
Species *Neohibolites minimus* (Miller, 1826)
Family OXYTEUTHIDAE Stolley, 1919
Genus AULACOTEUTHIS Stolley, 1911
Species *Aulacoteuthis speetonensis* (Pavlov, 1892)
Suborder BELEMNOPSEINA Jeletzky, 1965.
Family BELEMNITELLIDAE Pavlov, 1914.
Genus BELEMNELLOCAMAX Naidin, 1964
Species *Belemnellocamax mammillatus mammillatus* (Nilsson, 1826).

TABLE 3. Diagnosis of the material studied. L, total length of specimen; dtM, maximum transverse diameter measured in the dorsoventral aspect; and see Table 1

Species	Type material	Diagnosis
Cp	A lectotype has not been selected.	See Phillips 1865, pp. 113–120; Rogér 1952, pp. 716–717; Naef 1922, pp. 249–253. *Remarks:* (1) London Brick Company (LBC) pit, Stewartby; average L = 11·0 cm, SD = 1·8 cm, n = 17, average dtM = 1·2 cm, SD = 0·25 cm, n = 17 (2) LBC-pit NNW of Yaxley; average L = 11·1 cm, SD = 1·7 cm, n = 19; average dtM = 1·2 cm, SD = 0·2 cm, n = 19 (3) North Sea boreholes; only fractured specimens. (4) See text-fig. 2*a*.
Hh	Holotype. Described by Montfort, 1808, p. 387.	See Phillips 1865, pp. 111–113; Rogér 1952, pp. 714–715; Naef 1922, p. 244. *Remarks:* (1) Riegraf (1981, pp. 81–82) in his work on German specimens, recognizes 3 subgenera of the genus *Hibolithes* Montfort, 1808, and 4 subspecies of the species *Hibolithes* (*Hibolithes*) *hastatus* Montfort, 1808. According to Dr P. Doyle (*pers. comm.* 1984), the British Middle to Upper Jurassic belemnites are in need of revision, and no attempt is therefore made to differentiate subspecies in the present study. (2) Average L and dtM; (a) Tidmoor Point; 2·8 cm, SD = 0·5 cm, n = 4; 0·41 cm, SD = 0·07 cm, n = 4. (b) Warboys; 3·0 cm, SD = 0·3 cm, n = 5; 0·6 cm, SD = 0·45 cm, n = 6. (3) See text-fig. 2*b*.
As	*Lectotype*. Described by Swinnerton 1948, p. 52. British Museum (Natural History) No. C42865.	See Swinnerton 1948, pp. 46–52 and Mutterlose 1983, pp. 66–67. *Remarks:* (1) This specimen was fractured through the alveolar and apical regions. Consequently, only sections close to the protoconch, through the stem and part of the apical region could be examined. (2) The distinctive feature of the genus *Aulacoteuthis* Stolley is the presence of a median furrow which varies greatly in extent forwards and backwards and in its depth and width (Swinnerton 1948, p. 45). It is difficult to estimate the length of this furrow in my specimen. Swinnerton uses the length of this feature as a criterion to distinguish *A. ascendens* from *A. speetonensis*. According to Mutterlose (1983), however, it is not possible to differentiate these two species, and he therefore considers *A. ascendens* to be a synonym of *A. speetonensis*. Swinnerton moreover uses slimness of form to distinguish *A. ascendens* from *A. absolutiformes* (1948, p. 48). The slimness of form is indeed a characteristic feature of my specimen, and in this respect it conforms to the specimens depicted by Swinnerton (1948, pl. 13). Due to the slimness of form I prefer to ascribe my specimen to the species *Aulacoteuthis speetonensis*.

Table 3 (*cont.*)

Species	Type material	Diagnosis
		(3) The specimen was collected in the slipped beds of Speeton Clay at Speeton Beck, and the exact stratigraphic position is thus not recognized. Rawson (1972), however, recorded *Aulacoteuthis* sp. from a limited series of thin beds at the top of lower B and base of the Cement beds at Speeton. Pyrite along the ventral furrow of my specimen indicates that it probably originates from the LB2 bed, which contains highly pyritic clays (Neale 1974, p. 231, table 9). (4) L = 4·5 cm, dtM = 0·7 cm (fractured specimen). (5) See text. fig. 2*c*.
Ne	*Lectotype*. Swinnerton (1936–55, p. 65) selected the specimen figured by d'Orbigny 1847 (pl. 9, fig. 8) as the lectotype.	See Swinnerton 1936–55, pp. 64–66. *Remarks:* (1) The specimen presented to me did not have its alveolar part preserved, and the ventral furrow is consequently not visible. Lateral lines are weakly developed. The ventral margin has a gently convex curvature throughout its length which becomes markedly convex close to the apex. The apex is acute and symmetrical. Transverse sections are semicircular to circular. (2) L = 2·7 cm; dtM = 0·53 cm (fractured specimen) (3) The specimen has characters more compatible with *N. ewaldi* than with *N. minimus*. It is, however, found in the Red Chalk known for its high content of *N. minimus* (Wilson 1948, p. 63; Swinnerton 1936–55, p. 78; Neale 1974, p. 231, fig. 69). The specimen is more acute compared to the *N. minimus* of Mundays Hill and Double Arches. Cross-sections are semicircular throughout the stem region as opposed to the typical subquadratic to quadratic shape of the *minimus* types (Spaeth 1971*a*, pp. 59–60). On the other hand, acute forms of *N. minimus* are not uncommon (Swinnerton 1936–55, p. 73). Although this classification is a matter of dispute, I shall continue to refer to the specimen as *Neohibolites ewaldi*. (4) See text-fig. 2*d*.
Nm	*Lectotype*. Described by Swinnerton 1955, p. 72, figs. 8a–e. British Museum (Natural History) No. C44759.	See Spaeth 1971*a*, pp. 59–60 and Swinnerton 1936–55, pp. 71–74. *Remarks:* (1) Spaeth (1971*a*) recognizes 3 subspecies of *Neohibolites minimus*. No attempt is made in this study to make such a differentiation. (2) Average L of specimens from both pits; 2·6 cm, SD = 0·3 cm, n = 129. Average dtM = 0·45 cm, SD = 0·06 cm, n = 130. (3) The specimens from both pits probably originate from the upper part of the *Hoplites spathi* subzone (part of the *dentatus* zone) sediments, as these are known to contain numerous rostra of *N. minimus* (Owen 1972, p. 307). (4) See text-fig. 2*e*.

Table 3 (*cont.*)

Species	Type material	Diagnosis
Bm	According to Christensen (1975, p. 44) a lectotype has never been selected. He claims that the figures of Nilsson (1827) are good and quite sufficient for the recognition of the species.	(1) See Christensen 1975, pp. 44–46. (2) See text-fig. 2*f*.

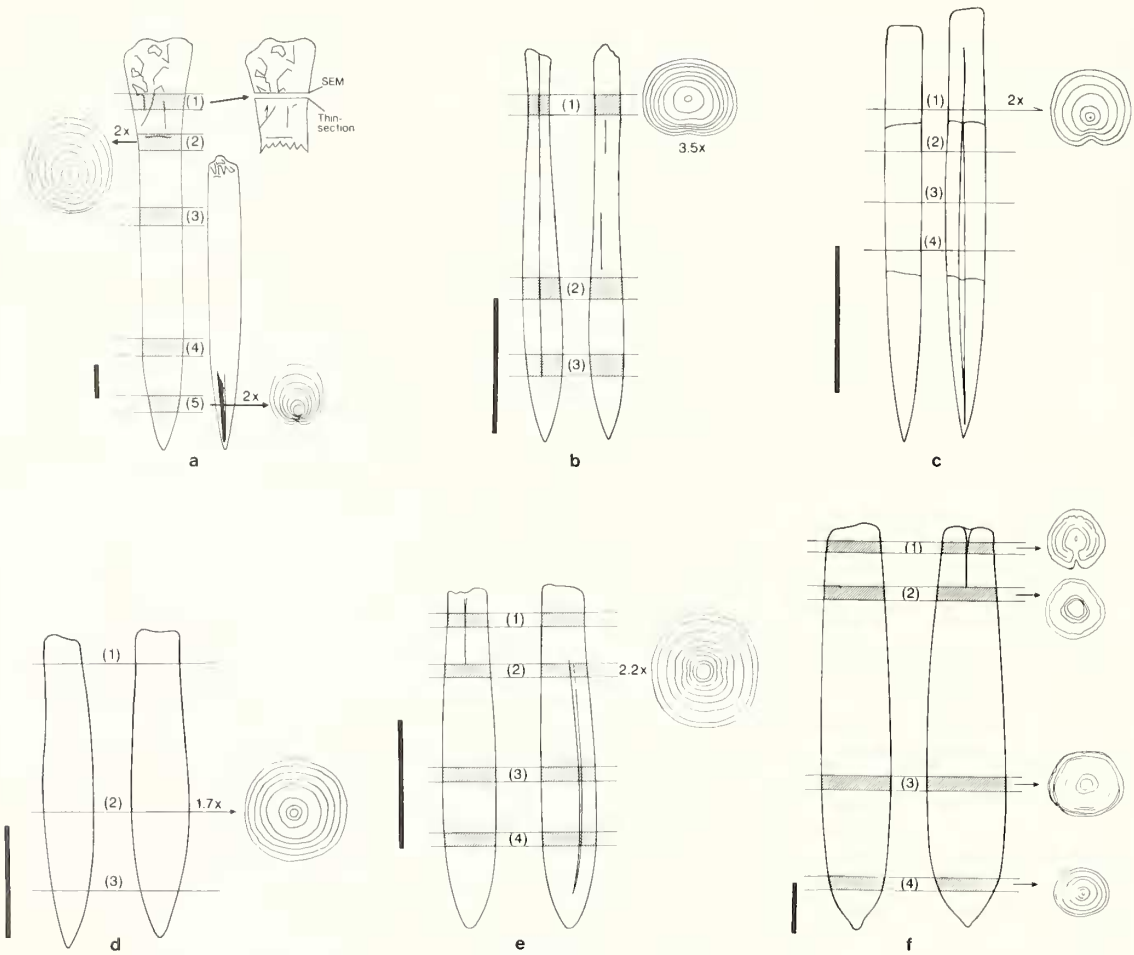

TEXT-FIG. 2. Position of cross-sections; *a*, *Cylindroteuthis puzosiana*, right lateral (left) and ventral (right) aspects of two specimens, opposing surfaces are prepared one for SEM, the other for thin-sectioning and subsequent inspection by means of ordinary transmitted light, cathodoluminescence and blue-light fluorescence microscopy; *b*, ventral (left) and right lateral aspect of *Hibolithes* (*H.*) *hastatus*; *c*, right lateral (left) and ventral aspect of *Aulacoteuthis speetonensis*; *d*, right lateral (left) and ventral aspect of *Neohibolites ewaldi*; *e*, ventral (left) and left lateral aspect of *N. minimus*; *f*, right lateral (left) and ventral aspect of *Belemnellocamax mammillatus mammillatus*; scale bars, 1 cm.

RESULTS

Preliminary assessment of preservation

A 'rough', preliminary assessment of the state of preservation of rostra was carried out by means of a binocular microscope (Table 4). Diagenetically altered zones were assumed to be recognizable as clearly recrystallized, translucent zones with no concentric structures (text-fig. 3D); and/or opaque, whitish zones with poorly defined growth-rings, though the latter in some cases seemed to have been accentuated by diagenesis (cf. Stevens and Clayton 1971, p. 869; text-figs. 3A–G).

Morphology of sections revealed by SEM study

The chemical reaction times necessary to reveal the concentric growth-ring patterns varied according to the type of medium used, (whether acid, oxidizing or fixing agent; Table 2), size of

TABLE 4. Preliminary assessment of preservation by means of examination under a binocular microscope; abbreviations, see Table 1

Species	Growth-rings	Opaque zones with poorly defined or accentuated growth-rings	Comments
Cp	Clearly discernible, alternating brownish and whitish rings.	Mostly confined to the central regions (around the alveolus and the apical region) and at the venter; text-fig. 3A.	The whitish rings are often discontinuous and generally thinner than the brownish ones (text-fig. 3A). Their discontinuous nature indicates a diagenetic origin. Clearly recrystallized, translucent zones are present in a few sections only.
Hh	Frequently visualized in the opaque zones, otherwise not as clearly defined as for Cp.	At the margins of adoral sections; text-fig. 3B.	Growth-rings are best defined in the stem sections (text-fig. 3C). Clearly recrystallized, translucent zones are present in a few sections only.
As	Clearly discernible, alternating brownish and whitish rings; text-fig. 3D.	Anterior sections close to the alveolus and at the ventral furrow.	Clearly recrystallized, translucent zones are present in a few sections only (text-fig. 3D).
Ne	Alternating diffuse whitish and brownish rings; text-fig. 3E.		The whitish rings are generally thicker compared to the other species.
Nm	Alternating whitish and brownish rings more difficult to visualize compared to the other species.	Around the alveolus; text-fig. 3F.	Preservation state is apparently very good.
Bm	Not clearly discernible, but can be accentuated in the opaque zones. The brownish calcite frequently shows thick but poorly defined growth-rings.	Adoral sections frequently show a whitish marginal zone which undulates towards the centre, and a distinct whitish zone around the apical line and pseudo-alveolus; text-fig. 3G.	Between the marginal and central whitish zone there is an area of brownish calcite. Sections through the stem region show the fewest diagenetic fabrics.

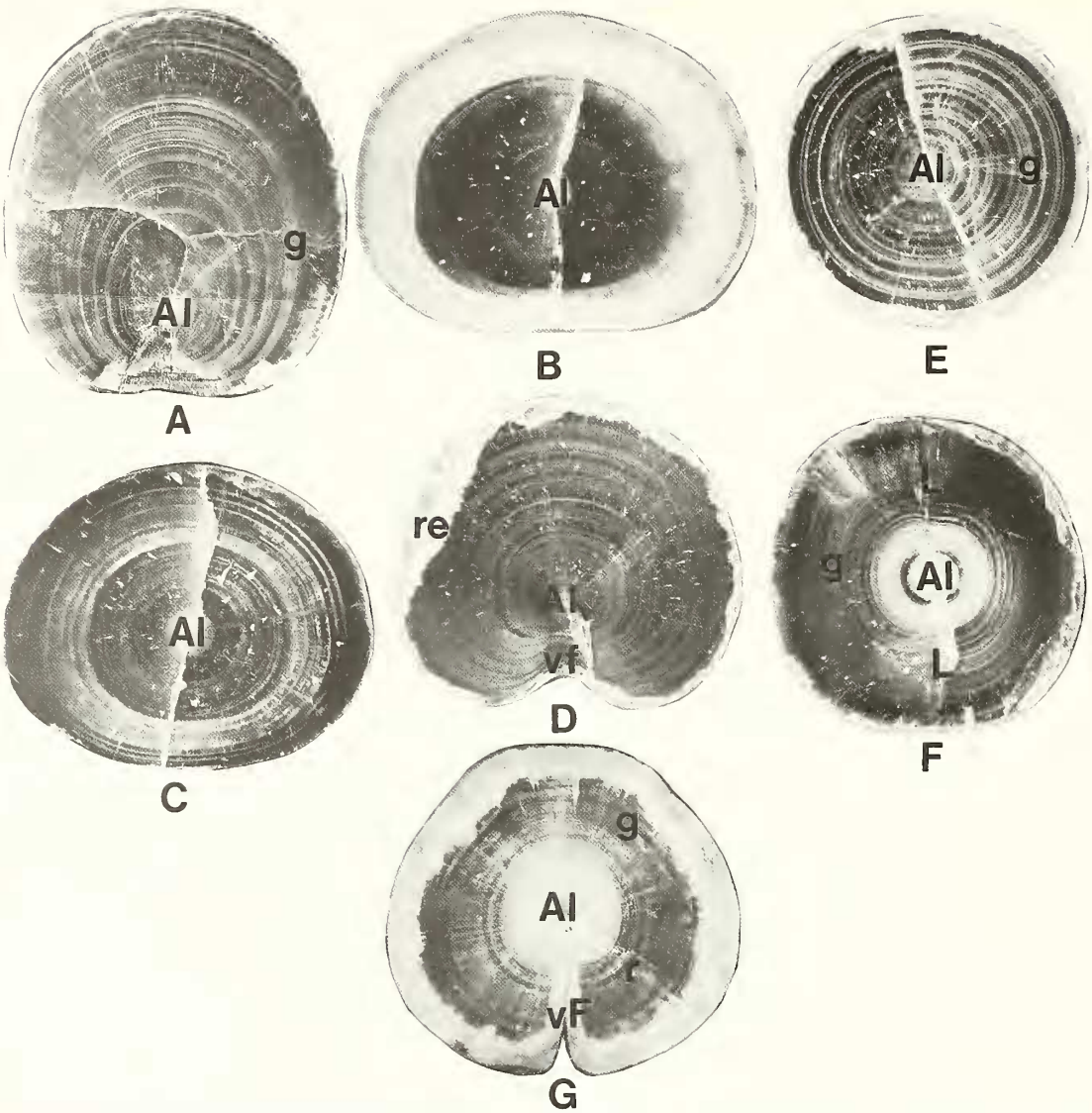

TEXT-FIG. 3. All photos of cross-sections under ordinary incident light (OIL). Al, apical line; vF, ventral furrow; dtM, maximum transverse diameter (cf. Stevens 1965); see also Table 3 and text-fig. 7; A, *Cylindroteuthis puzosiana* d'Orbigny, Middle Callovian, England, posterior part of stem region, ventral side faces downwards, note asymmetry of section (i.e. the apical line, Al, is closer to the venter), distinct whitish growth-rings (g) are present, ×3·3; B, C, *Hibolithes* (*H.*) *hastatus* Montfort, Lower Oxfordian, England, ventral side faces downwards; B, anterior part of stem region, note whitish zones around apical line (Al) and periphery, ×8·9; C, same specimen, section through the dtM, note that the whitish outer zone has disappeared, clearly defined whitish growth-rings are present, ×8·9; D, *Aulacoteuthis speetonensis* Stolley, Barremian, England; stem region, ventral side faces downwards, note asymmetry of section and recrystallized dorsolateral zone (re), ×4·6; E, *Neohibolites ewaldi* (v. Strombeck), Upper Albian, England; section through the dtM, ventral side faces downwards, note semicircular shape of cross-section, and distinct whitish rings (g), no lateral lines are visible, ×10·3; F, *N. minimus* (Miller), Middle Albian, England; close to protoconch, ventral side at left-hand side, note the subquadratic shape of section, lateral lines (L), diffuse whitish rings (g), and bright whitish zone around the apical line (Al), ×8·3; G, *Belemnellocamax mammillatus mammillatus* (Nilsson), Uppermost Lower Campanian, Sweden; alveolar region, ventral side faces downwards, note the heart-shaped section, whitish zones proximal to pseudoalveolus (Al) and at periphery, whitish discontinuous rings (g) and radial structures (r); ×4·3.

specimen, and position of section within the rostrum (whether alveolar, stem, or apical sections). Smaller specimens and alveolar sections generally needed the shorter exposure times. Optimal exposure times were determined by inspecting the slabs under a binocular microscope. Examination under a SEM prior to this stage failed to reveal more 'delicate' growth-rings. Investigation under a binocular microscope is a rapid and fairly reliable way to assure an appropriate degree of chemical etching, compared to the time-consuming inspection under SEM.

Dilute acids (Table 2) reveal growth-rings as alternating thin and thick layers, where the thin layers appear as microtopographic 'highs' (see Barskov 1970). This morphology is by and large common to all of the species studied (Pl. 84, figs. 1 and 2; see also text-fig. 10).

Hydrogen peroxide (Table 2) produces a similar, but 'negative' image (Pl. 84, figs. 3 and 5; cf fig. 4). The rounded crystal corners revealed by this medium are probably an effect of a 'transport-controlled' dissolution process (Berner 1980, p. 106). However, the organic acids produced would probably be weak and normally facilitate a 'surface reaction-controlled' dissolution process (Berner 1980, p. 106). Unfortunately, the pH of the reaction was not controlled, and thus it is difficult to interpret whether this fabric is due to diagenesis (cf. Al-Aasm and Veizer 1986) or simply to the dissolution process of calcite during treatment with the hydrogen peroxide.

Glutardialdehyde (Table 2) reveals growth-rings clearly (Pl. 84, figs. 6 and 7), and although radial structures are revealed as well, the expression is somewhat inferior to that produced by the other chemical media.

Summary of SEM results. Growth-rings were by and large recognizable under SEM after the application of etching, oxidizing and fixing agents. *H.* (*H.*) *hastatus* and *B. mammillatus* s.s. showed less defined rings compared to the other belemnite species (Pl. 85, figs. 1 and 2; Pl. 86, fig. 7).

Blue-light fluorescence microscopy of thin sections

The BL studies of belemnite cross-sections revealed growth-rings not visible under ordinary transmitted light (text-fig. 4A–D), and diagenetic features (text-figs. 4 and 5; see also Table 7). BLF reveals many more growth-rings than are normally apparent under a microscope (text-figs. 4B and D; text-figs. 5B and C). Growth rings of *H.* (*H.*) *hastatus* and *B. mammillatus* s.s., however, are generally more difficult to discern (text-fig. 4F; text-figs. 5A and D).

X-ray diffractometry

The mineralogy of the rostra studied was shown by XRD to be low-Mg calcite (text-fig. 6)

Total organic carbon analysis

This analysis was undertaken to demonstrate the existence of organic matter in the rostra (Table 5).

Diagenetic features

In this study diagenesis is considered to be physical and chemical post-mortem changes of belemnite shell parts, including dissolution, cementation and recrystallization. Organic diagenesis will only be briefly commented upon.

Scanning-electron microscopy. SEM studies revealed cements, as well as sediment-filled fractures and growth-rings (Pl. 84, figs. 6, 8 and 9; Pl. 85, figs. 1, 4 and 8; Pl. 86, figs. 1–3). In some cases, the effect of diagenesis is probably seen as a fusing of radial structures into more or less distinct and smooth 'tabular' growth-rings (Pl. 86, figs. 5 and 7, and see Barskov 1970, p. 559).

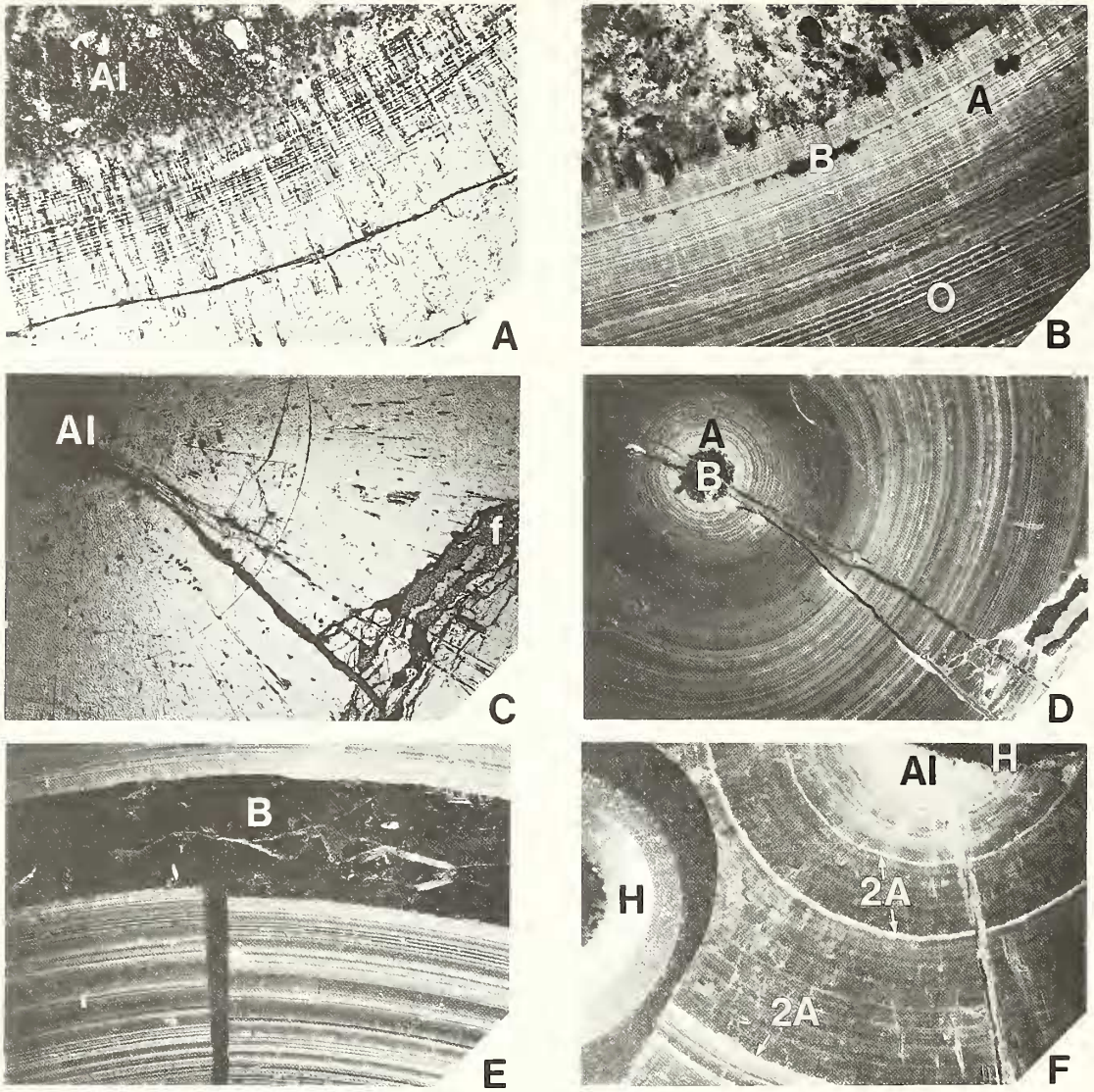

TEXT-FIG. 4. All photos of cross-sections. OTL, ordinary transmitted light; BL, blue-light fluorescence; see also text-fig. 7 and Table 3. A–E, *Cylindroteuthis puzosiana* (d'Orbigny), Callovian, England; A, alveolar section, ventral side close to the alveolus (Al); OTL, × 52; B, same section, BL; note laminar fluorescence of the original rostral fabric (o), 'type-A' is bright yellowish under BL (A), 'type-B' is non-fluorescent (B), compare Pl. 84, fig. 6 which is an SEM photo of the same section; C, anterior part of stem region, ventral side, OTL; f, fracture, × 20·8; D, same section, BL; note that the translucent part of apical region is non-fluorescent (B), whilst the opaque zone (OTL) is bright yellowish (A) under BL, notice also the numerous fluorescent growth-rings made visible; E, alveolar section, BL; the non-fluorescent cement (B) in this fracture system is bright luminescent under CL (type-B), × 52; F, *Hibolithes* (*H.*) *hastatus* Montfort, Lower Oxfordian, England; section through the dtM, ventrolateral side close to the apical line, BL; note the bright yellowish fluorescence of apical line area (Al) and of some prominent growth-rings (2A); H, borehole, × 52.

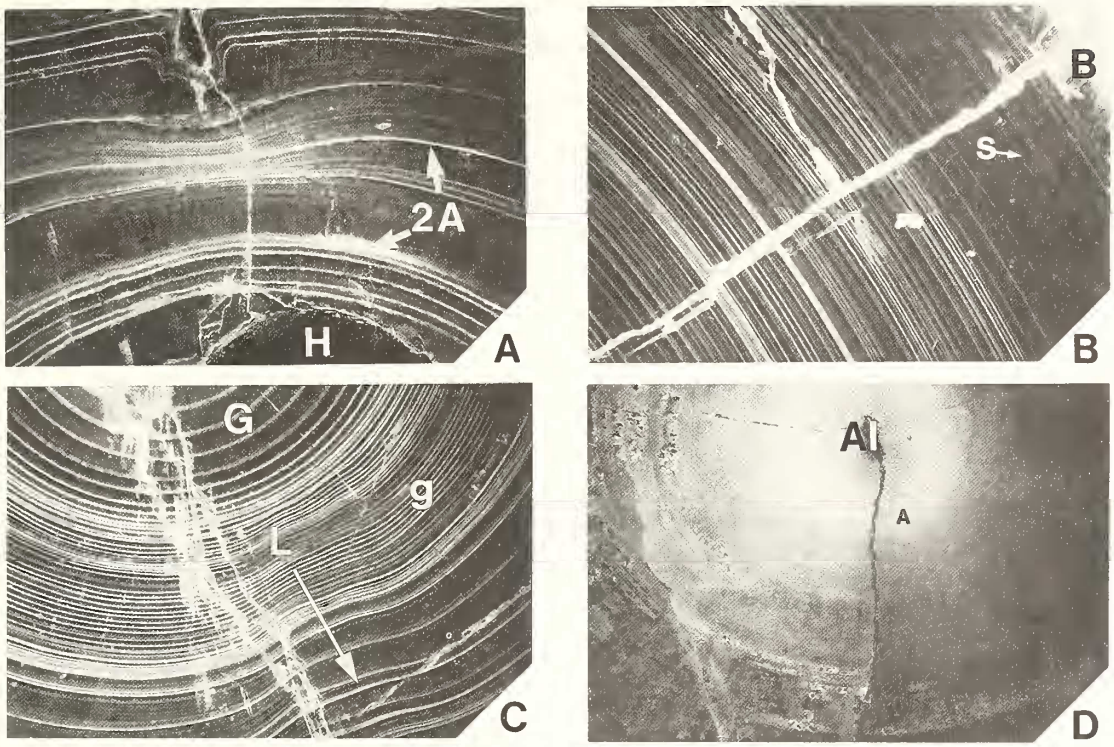

TEXT-FIG. 5. A, *Hibolithes* (*H.*) *hastatus* Montfort, Lower Oxfordian, England, dorsal side of specimen in text-fig. 4F; BL; the bright fluorescent laminae (2A) are bright luminescent under CL and opaque under OTL, compare text-fig. 7C; H, borehole, × 52; B, *Aulacoteuthis speetonensis* Stolley, Barremian, England; anterior part of stem region, at the periphery; BL; non-fluorescent zones (s) between radial structures are present in the outer region, but difficult to detect in a black and white print; growth-rings are also less fluorescent here; non-fluorescent rim cement (B, corresponds to type-B under CL), × 52; C, *Neohibolites minimus* (Miller), Middle Albian, England; right lateral side close to the apical line; note semi-circular thick growth rings (G) close to the apical line, and the asymmetric thinner ones (g) towards the periphery; L, lateral line; BL, × 52; D, *Belemnellocamax mammillatus mammillatus* (Nilsson), Uppermost Lower Campanian, Sweden; section through the dtM-region, apical line (Al) and ventrally; BL; note the 'diffuse' fluorescence (A, corresponds to type-A luminescence), × 52.

Cathodoluminescence. The majority of thin sections studied show reddish luminescence only in certain zones (Table 6):

(1) Fractures, which are often difficult to detect under ordinary transmitted light (OTL), and may be translucent, opaque, or even 'invisible' (text-fig. 7A and B).
(2) Growth-rings, some of which are continuous to discontinuous, brightly luminescent, and appear either as dark opaque bands (text-figs. 7A–C and F; 8A, B), or as translucent bands under OTL (text-fig. 7A); others are continuous to discontinuous, bright to dull luminescent, and seemingly invisible under OTL (text-figs. 7A–D).
(3) Radial structures which are luminescent along the edges, or as a whole, and are opaque, translucent or invisible under OTL (text-fig. 8D).
(4) Cements of the apical line and rim (text-fig. 7A–D).

The luminescent fabrics are referred to as:

(1) 'Type-A', which is opaque (OTL), bright reddish and sometimes bluish (CL).
(2) 'Type-B', which is translucent (OTL), bright reddish to reddish (CL).

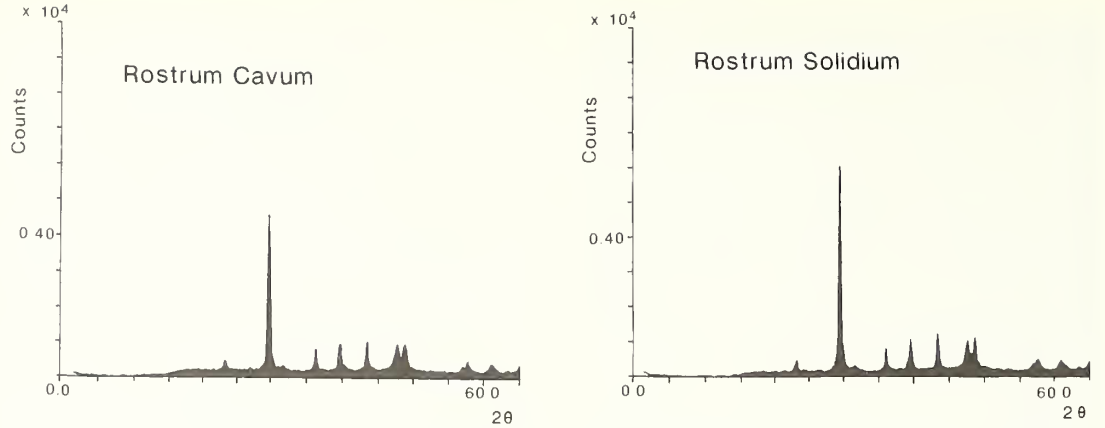

TEXT-FIG. 6. X-ray diffractograms of a *Cylindroteuthis puzosiana*; rostrum cavum and rostrum solidium.

TABLE 5. Analyses of total organic carbon (TOC) of ten cross-sectioned slabs of seven belemnite rostra. Cp1-1, alveolar section of *Cylindroteuthis puzosiana*; CpI-A and B, Cp3-3, Cp16, stem sections of three *C. puzosiana*; TP-I and II, stem sections of *Hibolithes* (*H.*) *hastatus* from Tidmoor Point; Nm-I and II, stem sections of *Neohibolites minimus*; Bm25, stem section of *Belemnellocamax mammillatus mammillatus*

Sample	TOC (ppm of 'whole rock')
CpI-A	33
CpI-B	44
Cp1-1	33
Cp3-3	69
Cp16	29
TP-I	580
TP-II	180
Nm-I	Traces
Nm-II	Traces
Bm25	88

(3) 'Type-C', which is 'invisible' (OTL), faintly reddish to reddish and sometimes bluish (CL). These features, however, are frequently difficult to recognize on black and white photographs.

Summary of CL results. All of the belemnite species studied show various luminescent features. *H.* (*H.*) *hastatus* and *B. mammillatus* s.s. both show numerous luminescing fabrics, whereas *C. puzosiana*, *A. speetonensis*, *N. ewaldi* and *N. minimus* generally exhibited fewer. In the latter four species, most of the luminescence was confined to an area around the alveolus and pseudoalveolus as well as the apical line. No luminescence was observed in the rostral substance adjacent to fractures (text-fig. 9).

As previously mentioned, BLF data also provide information about diagenesis, especially when combined with other data (Table 7). The type-A luminescent fabrics are bright yellowish under blue light, and invariably stain reddish. However, they show dull to very dull greenish to yellowish fluorescence in some cases (text-fig. 5D). The type-B luminescent fabrics, on the other hand, are invariably non-fluorescent, and stain bluish. Type-C luminescent fabrics are not distinguished under blue light, nor under OTL, and stain reddish. All sections stained reddish, with bluish colour confined to 'type-B' fabrics. *N. ewaldi* and *B. mammillatus* s.s. stained reddish only.

INTERPRETATION AND DISCUSSION

Interpretation of morphological features

Acid preferentially etches away the calcite-rich areas. Microtopographic 'highs' (text-fig. 10) thus represent organic-rich zones (laminae obscurae of Müller-Stoll 1936) or 'diagenetic' (e.g. iron rich) areas that are less easily attacked by weak acids. These 'highs' (organic rich laminae) correspond to 'lows' under hydrogen peroxide treatment. The fact that radial structures are clearly outlined by means of hydrogen peroxide points to the presence of organic matter between them (see also Spaeth 1975, p. 329). Interfaces between radial structures revealed by both hydrogen peroxide and weak acids can be correlated in some cases. These interfaces probably have a lower content of organic matter compared to those revealed by hydrogen peroxide only (Pl. 84, figs. 4 and 5). The distribution of organic matter is also evident from the BLF study (text-figs. 4 and 5), but interfaces between radial structures are not clearly recognizable; i.e. any organic material between radial structures probably gives a very weak signal, because only the concentric fluorescence pattern is apparent. Non-fluorescent (and apparently non-cemented) zones, however, may be encountered – particularly in the outer regions. These are probably devoid of organic matter (text-fig. 5B; Pl. 87, fig. 7).

As mentioned earlier, glutardialdehyde reacts with organic material, especially proteins. The exact reaction pattern is unknown, but the aldehyde groups most probably react with peptide bonds or $-NH_2$ groups of free amino acids (Iversen 1973).

Although proteins in fossil material are easily degraded, free amino-acids have been reported from belemnite rostra by several authors (see Drozdova 1969; Westbroek *et al.* 1979). The same is indicated by preliminary analyses made by the present author. Whether there are chemical components in the insoluble organic fraction (Table 5) that are capable of reacting with the glutardialdehyde is, however, unknown. The glutaric acid component more easily attacks the organic-poor zones, and the combined effects thereby produce more or less clearly discernible growth-rings, where the topographically high and thick layers are fixed by the aldehyde, and the low thinner layers are etched by the acid component (Pl. 84, figs. 6 and 7; Pl. 85, figs. 1–7; Pl. 86, figs. 1, 6 and 8; see also text-fig. 11). Prolonged etching, however, will lead to a shrinkage of the zones initially fixed by the aldehyde (text-fig. 12). This seemingly contradicts the observations by Müller-Stoll (1936, p. 176) and the present author's experiments with weak acids, where laminae pellucidae appear to be many times thicker than laminae obscurae (text-fig. 10). This difference can be accounted for by the following mechanism (text-fig. 13).

(1) Organic matter is distributed throughout the section, but the concentration varies along radial structures in a laminar fashion. A similar variation is observed in shells of modern molluscs (Grégoire 1972, p. 51).

(2) The aldehyde component will react with the organic material, particularly if the organic/inorganic ratio is high and suitable chemical compounds are available to react with the aldehyde groups.

(3) The glutaric acid will preferentially etch areas where the inorganic/organic ratio is high. The acid effect is particularly evident in zones where there is an abrupt change in the concentration of organic matter (Pl. 87, figs. 4 and 5).

Another fact worth mentioning is that the areas fixed by aldehyde are also observed along radial structures in some places (Pl. 85, fig. 6). These areas may contain remnants of organic material.

Diagenesis

All specimens subjected to XRD analysis showed invariably a low-Mg calcite mineralogy (text-fig. 6), and the majority showed no signs of obvious recrystallization (Table 4). One cannot conclude, however, that they were unaffected by diagenesis as this is contradicted by the CL data (Table 6; see also text-fig. 9). Fusion of growth-rings is recognizable in most specimens (Pl. 86, figs. 3, 5 and 7) and can often be correlated with reddish luminescence of type-A or -B (see earlier text). In those cases where fusion is not accompanied by luminescence, there are reasons to believe that the process

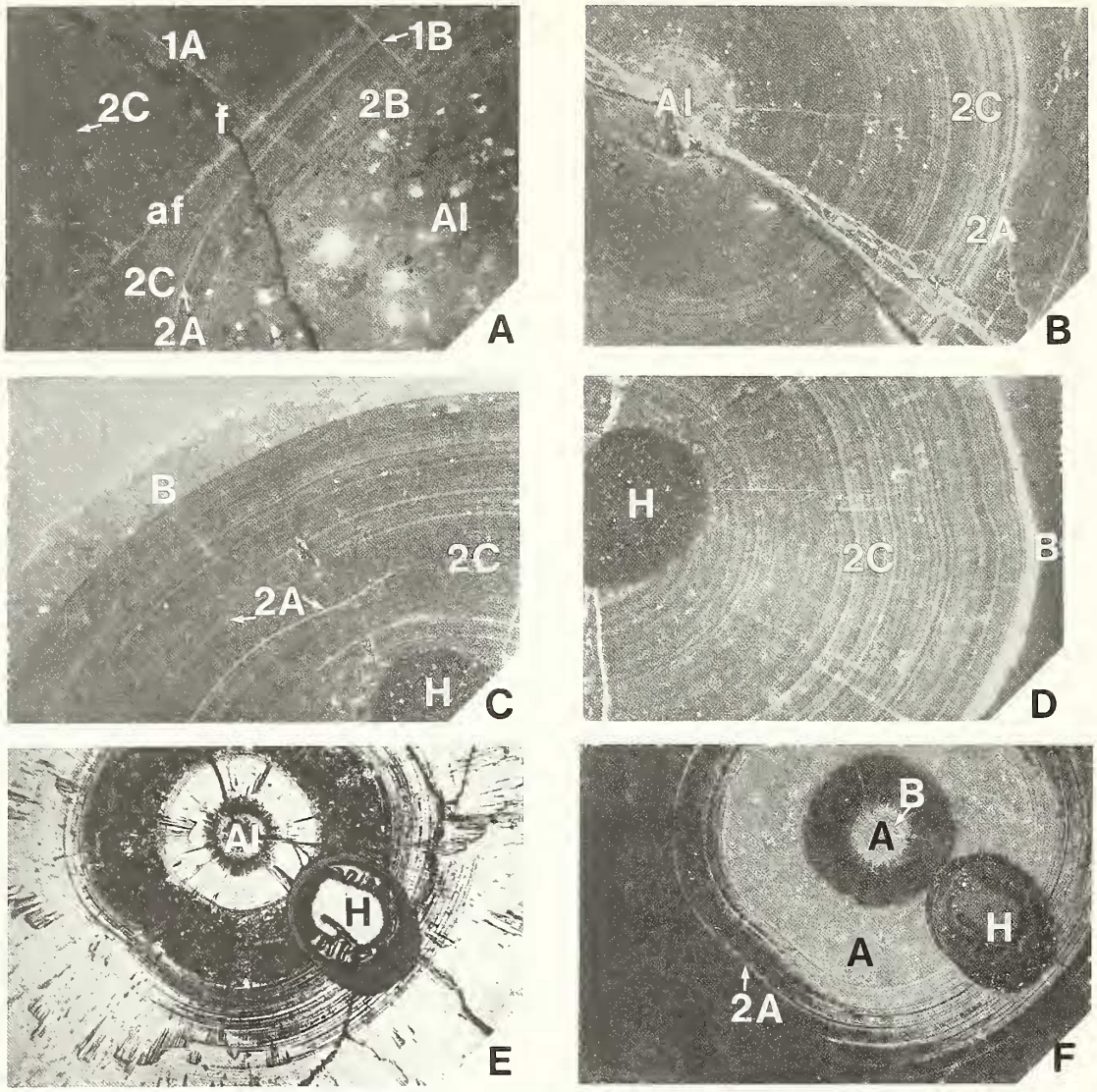

TEXT-FIG. 7. Unless otherwise specified, photos are of cross-sections. CL, cathodolumineseence; DF, dark field; A, type-A luminescence (including 1, fractures and 2, growth-rings); B, type-B lumineseence (ineluding 1, fractures and 2, growth-rings); C, type-C lumineseence (ineluding 1, fractures and 2, growth-rings). A, B, *Cylindroteuthis puzosiana* (d'Orbigny), Callovian, England; A, alveolar section proximal to sediment-filled alveolus (Al); CL, exposure time, 1 min.; note the many '2C' not deteetable under OTL, some of these are only faintly lumineseent, and eonsequently hard to deteet in a blaek and white print; note also the dark 'empty' fraeture (f), the '1B', '1A', '2A' and '2B'; the artificial fraeture, i.e. preparation artifaet (af) is light bluish, and shows a bright yellowish fluoreseenee, ×23; B, stem section, apical line area, ventral side; CL, exposure time, 8 mins. (DF); note bright lumineseent rings ('2A', '2C') elose to the ventral surfaee, and 'type-B' of the apieal line (Al), ×51; C, D, *Hibolithes* (*H.*) *hastatus* Montfort, Callovian and Lower Oxfordian, England; C, seetion through dtM, dorsal side; Cl, exposure time, 2 mins.; notiee elearly diseernible '2A' and '2C', some of whieh are buekled; note also the lumineseent rim eement (B, type-B), ×26·8; D, anterior part of stem region; CL, exposure time, 5 mins.; note elearly lumineseing rings ('2C') and rim eement (B, type B); eompare Pl. 85. figs. 1 and 2, whieh show the same seetion in a ventral aspeet; the more diffuse expression of growth-rings might be due partially to a diagenetie modifieation of the low-Mg ealeite skeleton; H, borehole, ×26·8; E, F, *Neohibolites minimus* (Miller), Middle Albian, England; E, elose to protoeoneh, OTL; note the opaque sediment-filled zone around the apieal-line area (Al), ×26·8; F, same seetion; CL, exposure time, 5 mins.; note the 'type-A and -B' (A, B) of the apical line and sediment-filled zone; compare Pl. 86, fig. 2 whieh shows the same seetion under SEM.

TABLE 6. Ranking of the amount of luminescent fabrics and dominant luminescent types among the different species. 2A, B and C, luminescent growth-rings of type-A, -B and -C; see also Table 1

Species	Amount of luminescing features; ranking (1 = highest amount)	Dominant luminescence types
Cp	3	Frequently dominated by '2A' and '2C' in the alveolar sections. '2A' dominates ventrally in the apical sections; text-fig. 7A, B.
Hh	1	Most sections dominated by '2C' and '2A'; text-fig. 7C, D.
As	4	As for Cp, but ventral luminescence less pronounced.
Ne	6	As for Nm, but generally less reddish luminescence. '2C' and occasionally '2A' are bluish
Nm	5	'2A' generally confined to area close to the alveolus; text. fig. 7E, F; 8A, B.
Bm	2	Type-A of growth-rings in peripheral zones, around the apical line and alveolus, as well as along radial structures; text-fig. 8C, D.

TABLE 7. Correlation of fabrics as seen under CL, cathodoluminescence; BL, blue-light fluorescence; OTL, ordinary transmitted light; OIL, ordinary incident light; and by means of staining

CL	BLF	OTL	OIL	Staining
Type-A	Bright yellowish	Opaque	Whitish	Reddish
Type-B	Non-fluorescent	Translucent	Translucent	Bluish
Type-C	Not distinguished	'Invisible'	'Invisible'	Reddish

was an early diagenetic effect of the marine environment (see Wilkinson 1982, pp. 198–203; Sandberg 1985; Al-Aasm and Veizer 1986) or possibly even an *in vivo* process (Hückel and Hemleben 1976, p. 364). *H.* (*H.*) *hastatus* and *B. mammillatus* s.s. showed extensive diagenetic alterations in the alveolar region (text-figs 3B, G; compare text-fig. 8C). This diagenetic pattern was probably controlled by the original morphology, as it has been encountered in all specimens of these two species. They all show relatively thick and poorly defined growth increments related to the early ontogenetic stages, and thinner, more easily recognizable rings of later origin. The products of these later stages were frequently susceptible to diagenesis (Pl. 85, fig. 1; Pl. 86, fig. 7). The similarity of growth-ring pattern in these two species, and the fact that they originated from different sedimentary environments (Table 1), further support the notion that their original rostral structure controlled the pattern of diagenetic alteration.

Type-A and -B luminescent features. These diagenetic features (text-figs. 7, 4E) are probably the result of differential dissolution and cementation of the rostrum. The translucent (type-B) zones invariably stain bluish, and may represent a cement formed in or below the sulphate-reduction zone

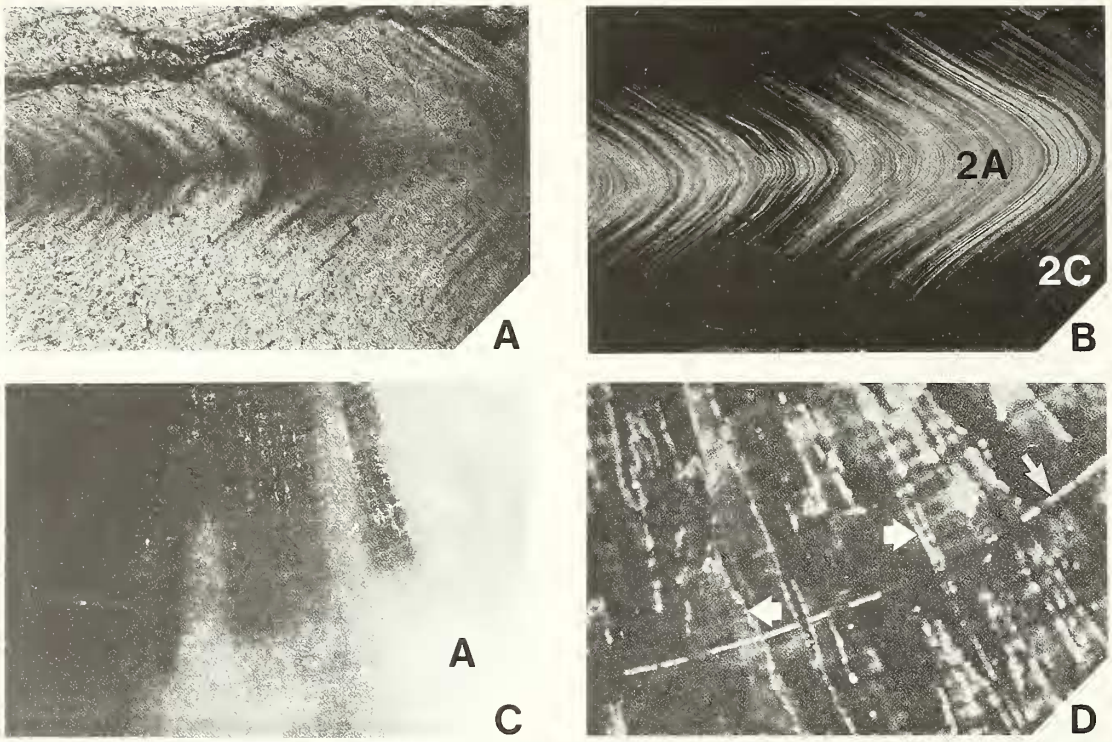

TEXT-FIG. 8. A, B, *Neohibolites minimus* (Miller), Middle Albian, England. Abbreviations; see text-figs. 4, 7. A, longitudinal section close to the apex, OTL; note the opaque zone which make up the apical line, ×26·8; B, same section; CL, exposure time, 6 mins.; notice the bright reddish 'type-A and -C' of the apical portion of growth-rings; C, D, *Belemnellocamax mammillatus mammillatus* (Nilsson), Uppermost Lower Campanian, Sweden; C, alveolar section, right lateral side close to the periphery; CL, exposure time, 50 secs. (DF); notice the 'type-A' of the 'structureless' undulating outer zone (compare text-fig. 3G), ×51; D, stem section, dorsolateral side $\frac{2}{3}$ the distance from apical line towards periphery; CL, exposure time, 6 mins. (DF); note the 'type-A' along radial structures and growth-rings (arrows), ×51.

(Hudson 1978; Curtis 1980, pp. 192–193; 1987). The fact that the blue-stained zones are bright reddish under CL, probably indicates that beside their high iron concentration (see Oldershaw and Scoffin 1967), these zones also contain manganese (see Nickel 1978; Pierson 1981; Frank *et al.* 1982; Fairchild 1983; ten Have and Heijnen 1985; Machel 1985; Mason 1987). The

EXPLANATION OF PLATE 84

Figs. 1–9. *Cylindroteuthis puzosiana* (d'Orbigny), scanning-electron micrographs. Callovian, England. Unless otherwise specified, gun voltage is 25 kV and photos are of cross-sections. 1, concentric growth-rings of the anterior part of stem region; 1% HCl, 3 mins; gun voltage, 10 kV. ×200. 2, detail of fig. 1, showing growth-rings (g) and radial structures (r). ×1000. 3, part of ventrolateral side of stem section halfway between the apical line and periphery; 35% H_2O_2, 48 hrs. ×76. 4, apical line area of stem section; 1% HCl, 3 mins.; d, diagenetic fabrics ('type-A'). ×100. 5, section shown in fig. 4; 35% H_2O_2, 48 hrs.; c, contaminant. 6, growth-rings close to sediment-filled alveolus (Al); 25% glutardialdehyde, 6 hrs.; d, diagenetic fabrics (including both 'type-A and -B'). ×76. 7, detail of fig. 6, showing radial structures (r) and growth-rings; i.e. topographic high (TH) and low (TL) layers. ×3784. 8, alveolar section showing cemented fractures (f); 25% glutardialdehyde, 10 hrs.; the cement is bright reddish under CL ('type-B'). ×76. 9, apical section close to the ventral furrow (vf); 25% glutardialdehyde, 16 hrs.; d, diagenetic fabrics ('type-A'), dark part of fracture is filled with mounting medium (M). ×34·4.

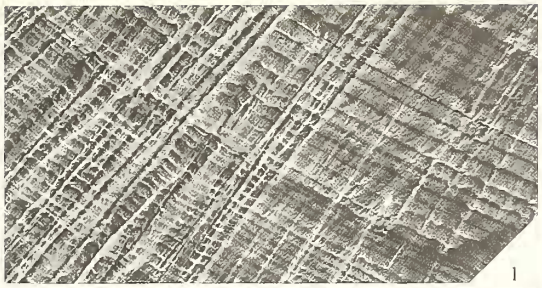
1

2


3

4

5

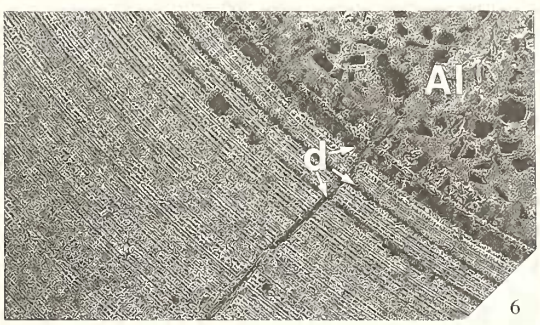

6

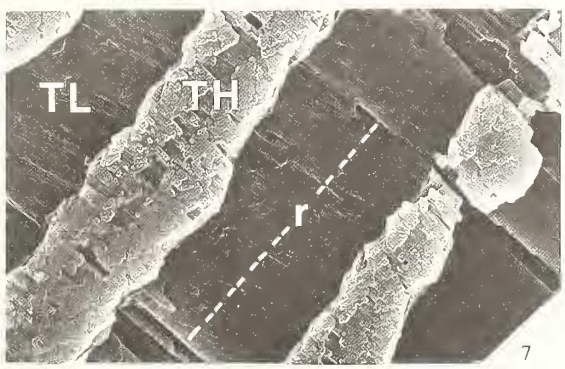

7

8

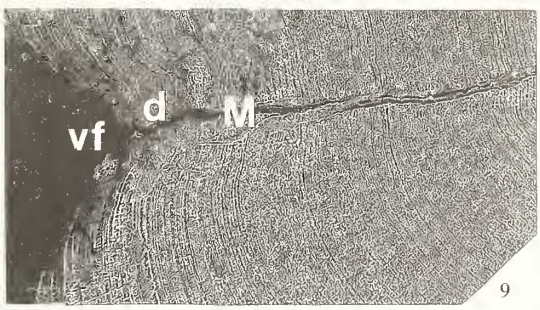

9

SÆLEN, *Cylindroteuthis puzosiana*

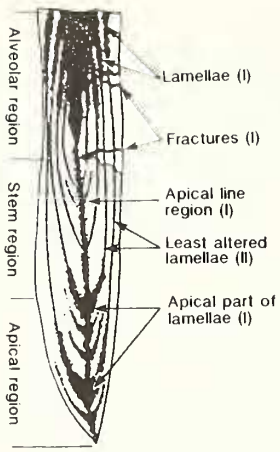

TEXT-FIG. 9. Schematic luminescence pattern for Cp, As, Ne and Nm; I, bright reddish luminescence; II, faint reddish luminescence. Abbreviations; see Table 1 (Fig. from Sælen and Karstang 1989.).

concentrations of Fe^{2+} and Mn^{2+} and their ratios, however, have not been systematically evaluated in the present study.

The type-A features are more difficult to explain, but may be due to a differential recrystallization of the rostrum (see Al-Aasm and Veizer 1986). The bright yellowish fluorescence of these zones, compared to the weaker fluorescence of presumed original rostral material, may indicate that organic matter in these zones has been altered by diagenetic fluids. As most of the sedimentary environments involved are known for their rich biogenic content (Casey 1966; Duff 1975), another explanation might be that organic molecules have been incorporated from the sediments during diagenesis.

As various trace elements are able to evoke fluorescence, the variation in the intensity of fluorescence could, of course, be ascribed partly to differences in the inorganic content. However, all of the sections studied show relatively high fluorescence intensity across their surfaces (though weaker than the diagenetic type-A fabrics) and the intensity of fluorescence of many organic substances is known to be very strong (cf. van Gijzel 1979, p. 11). Accordingly, it is reasonable to infer that at least the 'non-diagenetic' patterns observed under BLF are due to a primary variation in organic content within the rostra (see Dravis and Yurewicz 1985, p. 796 and pp. 802–803).

EXPLANATION OF PLATE 85

Figs. 1–3. *Hibolithes* (*Hibolithes*) *hastatus* Montfort, scanning-electron micrographs. Callovian and Lower Oxfordian, England. Unless otherwise specified, gun voltage is 25 kV, and photos are of cross sections. 1, anterior part of stem section, ventral side faces downwards; 25% glutardialdehyde, 5 hrs.; note the late asymmetrical growth stage (As) and the diagenetic fabrics (d, 'type-A'). ×76. 2, detail of growth-rings in fig. 1; notice the thin and less distinct rings (g) which make up a larger one (G); these rather 'diffuse' growth-rings (cf. fig. 3) are probably the result of a diagenetic modification of the low-Mg calcite skeleton (cf. text-fig. 7D). ×378·4. 3, close-up of growth-rings in the anterior part of stem section. ×3784.

Figs. 4, 5. *Aulacoteuthis speetonensis* Stolley, Barremian, England. 4, stem region, ventral side with furrow (vf) facing downwards; 25% glutardialdehyde, 6 hrs.; note the lateral lines (L) and fracture (f) filled with mounting medium. ×34·4. 5, stem section, close-up of growth-rings. ×3784.

Figs. 6, 7. *Neohibolites ewaldi* (v. Strombeck), Upper Albian, England. 6, growth-rings of anterior part of stem section; 25% glutardialdehyde, 5 hrs.; note the inter-radial zone (arrow) fixed by aldehyde. ×344. 7, section through the maximum transverse diameter, close-up of growth-rings; 25% glutardialdehyde, 6 hrs ×3784.

Fig. 8. *Neohibolites minimus* (Miller), Middle Albian, England. Longitudinal section close to the alveolus (left); 25% glutardialdehyde, 5 hrs., pre-etched with 5% acetic acid, 20 secs.; note the diagenetic fabrics (d, 'type-A'). ×378·4.

2

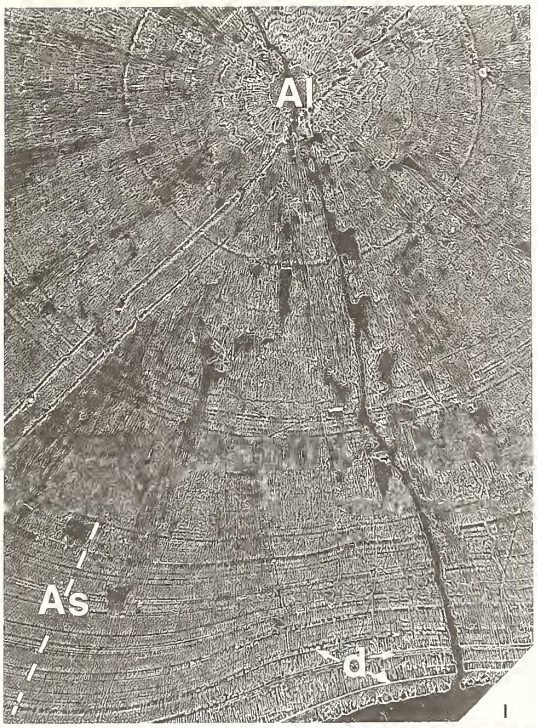

1

3

5

7

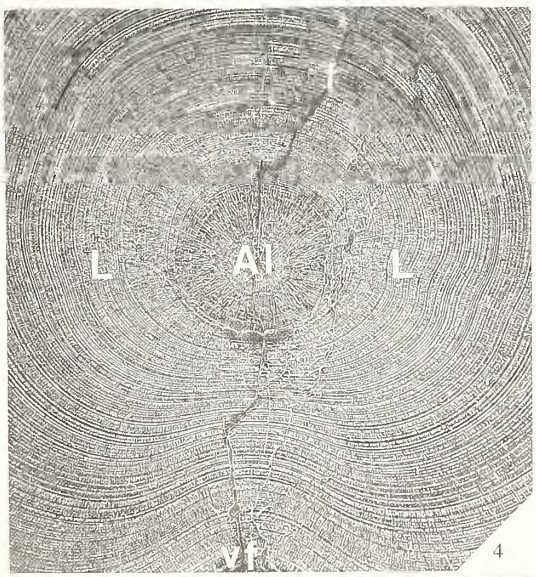

4


6

8

SÆLEN, *Hibolithes*, *Aulacoteuthis*, *Neohibolites*

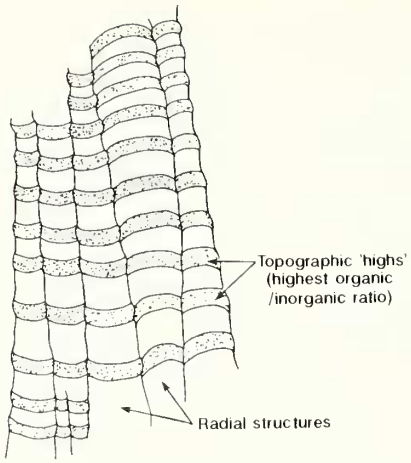

TEXT-FIG. 10. Radial structures and growth layers depicted by etching with weak acids.

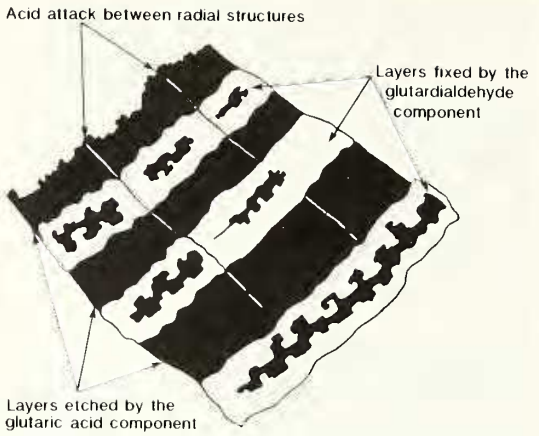

TEXT-FIG. 11. Treatment with 25% glutardialdehyde, pH ~ 4·0.

Type-C luminescent features. This luminescence is not easily correlated with either SEM or BLF features. However, when inspected under SEM, *B. mammillatus* s.s. and *H.* (*H.*) *hastatus* in some cases reveal radial structures seemingly stuck on top of one another. This fabric is correlated with type-C luminescence (Pl. 85, fig. 2; cf. text-fig. 7D). This type of luminescence may be attributed to thin coatings of syntaxial cement on the biogenic crystals (Bathurst 1975), although such cements could not be distinguished in the present study. On the other hand, it may be attributed to a differential recrystallization along the edges of crystals. The low-Mg calcite, despite its relative stability, sometimes suffers differential recrystallization which causes fusing of micro-structural units and rounding of prism corners (Al-Aasm and Veizer 1986, p. 142). A similar, partially diagenetic modification has been advocated for belemnite rostra by other authors (Veizer 1974). According to Ragland *et al.* (1979), however, diagenetic changes in the elemental composition of mollusc shells are even possible prior to apparent recrystallization, though no explanation is given as to what mechanisms are involved.

EXPLANATION OF PLATE 86

Scanning-electron micrographs of cross-sections. Unless otherwise specified, gun voltage is 25 kV. Abbreviations see text-fig. 3, and Plate 85.

Figs. 1–6. *Neohibolites minimus* (Miller), Middle Albian, England. 1, close to protoconch, ventral side faces downwards and slightly towards the right; 25% glutardialdehyde, 5 hrs., pre-etched with 5% acetic acid, 20 secs.; note the cemented apical line area (Al, 'type-B') and the fused 'type-A' growth-rings (d) ×76. 2, close to protoconch; 25% glutardialdehyde, 5 hrs., pre-etched with 5% acetic acid, 20 secs.; note the diagenetic fabrics; A, cement of the apical line area (large arrow); B, dissolved laminae filled with sediment and later cemented by low-Mg calcite (little arrow). ×34·4. 3, close-up of layers depicted in fig. 1; d, 'type-A' growth-rings; c, contaminant. ×34·4. 4, detail of Pl. 85, fig. 8; r, radial structure; g, growth-rings. ×1720. 5, growth-rings close to the alveolus; 25% glutardialdehyde, 5 hrs., pre-etched with 5% acetic acid, 20 secs.; note that this structure apparently resembles the 'palisade and septa' construction of the *Sepia* cuttlebone, compare text-fig. 19; r, radial structues; d, fabrics modified by diagenesis ('type-A'). ×1720. 6, stem region; 25% glutardialdehyde, 5 hrs., pre-etched with 5% acetic acid, 20 secs.; close-up of growth-rings. ×3440.

Figs. 7 and 8. *Belemnellocamax mammillatus mammillatus* (Nilsson), Uppermost Lower Campanian, Sweden. 7, dorsal aspect of stem section; 25% glutardialdehyde, 11 hrs.; notice the peripheral diagenetic zone (d, 'type-A'); fu, fused radial structures. ×76. 8, growth-rings of apical region; 25% glutardialdehyde. 11 hrs. ×3784.

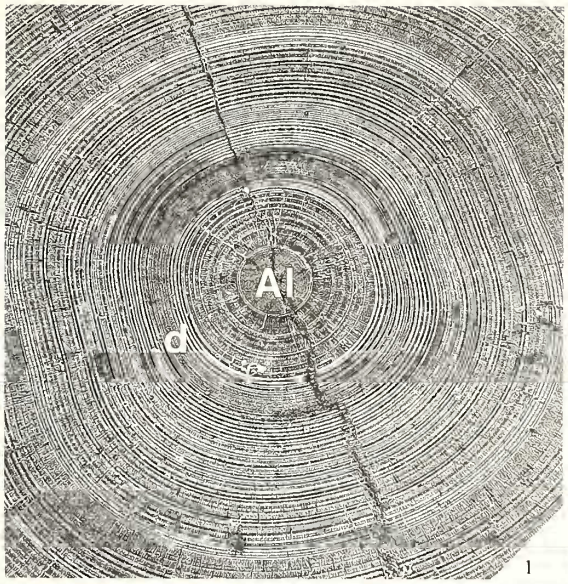

1


2

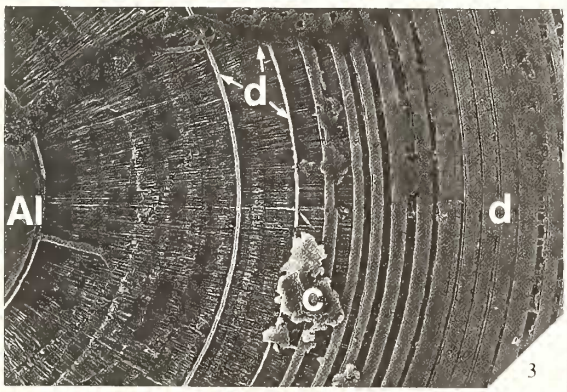

3

4

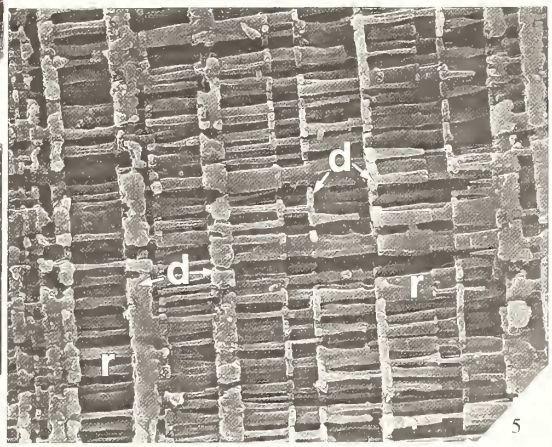

5

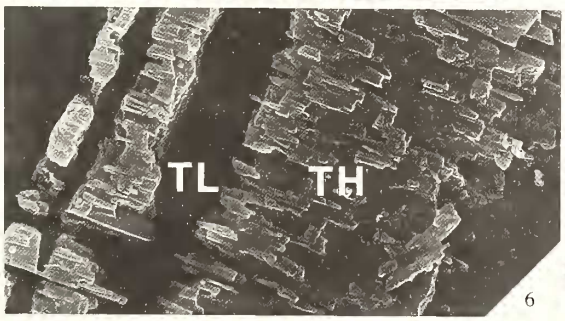

6

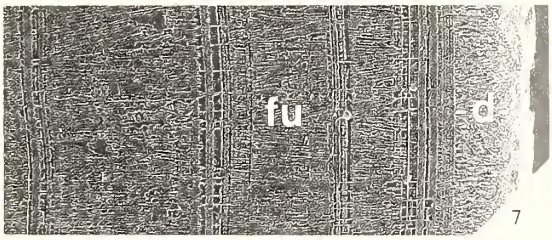

7

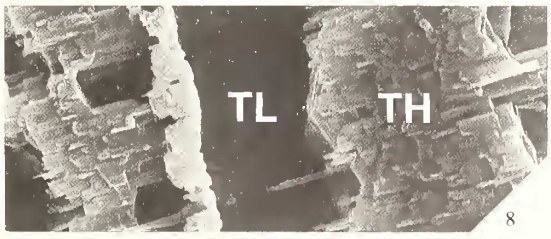

8

SÆLEN, *Neohibolites*, *Belemnellocamax*

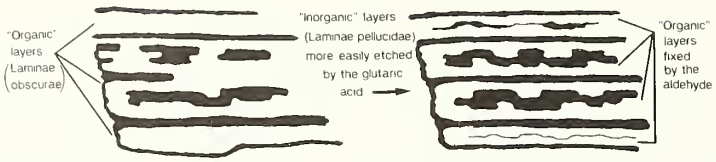

TEXT-FIG. 12. Treatment with 25% glutardialdehyde; effect of reaction time; left, incipient stage; right, later stage; only layers most strongly fixed by the aldehyde are preserved as topographic 'highs'.

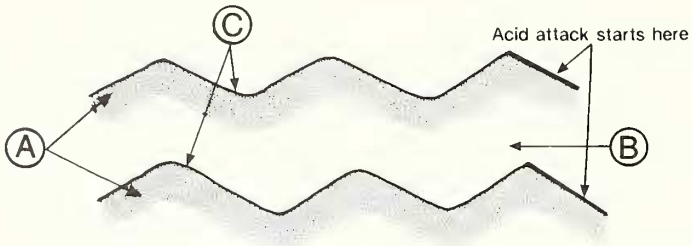

TEXT-FIG. 13. Schematic figure showing incipient attack by weak acids; A, 'organic-rich' layers; B, also contains organic matter, but the concentration is lower; C, abrupt change in concentration of organic components fixed by the aldehyde.

In this context, it is worth considering that if low-Mg calcite was stable in sea water during the late Jurassic and Cretaceous (see Wilkinson 1982; Sandberg 1985), a marine cementation of the rostra might be difficult to detect. Such a cement would not be expected to luminesce (cf. Veizer 1983, Table 3–3, p. 3–14; Machel 1985, p. 142), but it might be fluorescent (cf. Dravis and Yurewicz 1985, p. 800) and thus may not differ from the biogenic calcite of the rostrum.

Original mineralogy

The original mineralogy of the rostra studied is thought to be low-Mg calcite, and the supporting arguments are as follows.

(1) All of the specimens, in the 'non-luminescent' parts of their rostra (partly including the Type-C faint reddish rings), have an orderly structure composed of radial and concentric elements. It is hard to envisage that an original aragonitic rostrum would consistently preserve this fabric when transformed into low-Mg calcite (Sandberg 1983). The rostra could, of course, have been composed of high-Mg calcite, but no data from this study confirm the existence of present or former high-Mg calcite skeletal parts. In particular:
   (A) the XRD-data (text-fig. 6) do not support such a mineralogy, as the d-values around 3·03 indicate low-Mg calcite (see also Chave 1952),
   (B) no microdolomite has been observed (see also Richter and Füchtbauer 1978, p. 844), and
   (C) although Richter and Füchtbauer (1978) claimed that ferroan calcitic fossils with preserved microfabrics were originally composed of high-Mg calcite, the specimens studied here did not stain bluish except in certain clearly cemented zones (see above). The fact that high-Mg calcite has not been found in modern cephalopods (Bathurst 1975) also makes it difficult to infer such a mineralogy for belemnite rostra.

(2) The majority of specimens come from clay sequences (the Gault Clay and Oxford Clay) known to contain abundant, well-preserved, aragonitic fossils (see Hall and Kennedy 1967, pp. 383–384). It is thus feasible that an aragonitic rostrum would have easily survived under these conditions. The additional fact that aragonitic phragmocones are found in the same sediments adds further support to the interpretation that the majority of belemnite rostra were originally calcitic (see also Sandberg 1983; Brand and Morrison 1987).

In this context, it can be argued that the aragonite found in the rostrum cavum of a specimen of *N. minimus* from the Gault Clay, Folkestone (see Spaeth 1971*b* and 1973), does not necessarily indicate that all belemnite rostra were originally composed of this mineral. Other explanations are possible to account for the occasional aragonite rostra reported in the literature (see also Barskov 1970). In modern Mollusca, shell regeneration may lead to changes in the organic matrix composition, as well as in crystal type and mineralogy (Wilbur 1972, p. 131) and shells may originally be of bimineral composition (Spaeth 1973, p. 166). Although bimineral shells are common in the phylum Mollusca, no modern squids show such a phenomenon, and consequently the first explanation is more likely to account for the aragonite in the rostral parts of (at least) the *N. minimus* from Folkestone.

Diagenetic history

The shell matrix of modern molluscs is both inter- and intra-crystalline, and consists mainly of proteins (Wilbur 1972; Lutz and Rhoads 1980). As mentioned earlier, proteins of fossil material are easily degraded, and in a low-Mg calcite skeleton this can be expected to affect the intercrystalline material first. A degradation of intercrystalline organic material in belemnite rostra probably started early in their post-mortem history (see Tan and Hudson 1974, p. 108; Bayer 1975, p. 22), and might have increased the original porosity or created porous zones. The CL patterns (text-fig. 9) show that the diagenesis in most cases proceeded in a laminar fashion, which indicates a differential stability of laminae. In the alveolar sections and ventral layers of distinctly asymmetrical species (especially where furrows are developed as in *Cylindroteuthis puzosiana* and *Aulacoteuthis speetonensis*), growth-rings are relatively thin (see text-figs 3A, D; Pl. 84, figs. 6 and 9; Pl. 85, fig. 4; see also Swinnerton 1936, p. 14). A degradation of intercrystalline organic matter in such cases might have increased the surface area and thereby eased the actions of diagenetic fluids (see also Stevens and Clayton 1971, p. 873; Spaeth *et al.* 1971, p. 3148). There might, of course, also have been originally porous zones not totally filled with organic material (see Pl. 87, fig. 7). The fluorescence of presumably original biogenic material indicates, however, that such a porosity was probably of minor importance (see also Bandel *et al.* 1984). The amount of diagenetic change in these sections might, therefore, partly be ascribed to variations in permeability created during differential degradation of intercrystalline organic material.

As regards the relative time sequence in the present case, the patterns of laminescence of type-A and -C apparently predate the ferroan cement. The blue-stained fractures transect growth-rings of type-A and -C, and often make a contiguous system with blue-stained, cemented laminae (Pl. 84, fig. 8; text-fig. 4E).

Spaeth *et al.* (1971, p. 3148) found variation in $\delta^{18}O$ and $\delta^{13}C$ between rostra cava and rostra solida, although they could not distinguish whether this effect was due to metabolic or diagenetic processes. In the context of the present study, this difference can be understood better in terms of the CL patterns, and is thus ascribed to a diagenetic effect (Sælen and Karstang 1989).

The apical line has been claimed by several authors to be semipermeable, allowing solutions to percolate (Sturz-Köwing 1960, p. 61; Stevens and Clayton 1971, p. 834). Bandel *et al.* (1984, p. 287) observed, in a study on well preserved *Hibolithes* sp., that the apical line was formed by a radial growth of calcite prisms which they claimed had been connected to organic fibres. Spaeth (1971*a*, p. 24) ascribed the inferior stability of the apical line to the orientation of crystals in this zone. The frequently observed bright reddish luminescence of the apical line might therefore be ascribed to a change in size and morphology of radial structures; they decrease in size from the periphery towards the apical line area. Moreover, radial structures are thin and nearly parallel in the alveolar region, and become thicker and fan-like in the apical region (text-fig. 14). These changes in morphology and size probably eased the breakdown of intercrystalline organic material, and may partially explain the increased diagenetic effects in this region.

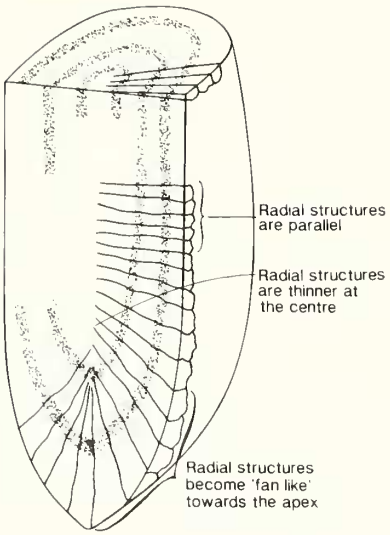

TEXT-FIG. 14. Change in size and morphology of radial structures along a schematic rostrum.

Construction of belemnite rostra

Based on the results obtained from the various chemical treatments (Table 2) and examination of thin sections under CL and BLF, the following model for the construction of belemnite rostra (not including the primordial rostrum) is proposed. The rostrum is made up of composite radial structures which accreted periodically to give a pattern of concentric growth-rings (text-fig. 15; Pl. 87, fig. 8). This pattern is recognized under BLF as more or less fluorescent growth-rings, and indicates that radial structures consists of growth increments with varying amounts of organic matter (text-figs. 15 and 16; Pl. 84, fig. 2; Pl 87, fig. 8; text-figs. 4 and 5). The existence, and varied distribution, of organic matter are further indicated by TOC analysis and treatment with hydrogen peroxide and glutardialdehyde.

The 'split' or 'indented' radial structures, seen particularly well in thin sections under crossed

EXPLANATION OF PLATE 87

Scanning-electron micrographs. Unless otherwise specified, photos are of cross-sections, and gun voltage is 25 kV.

Fig. 1. *Belemnellocamax mammillatus mammillatus* (Nilsson), Uppermost Lower Campanian. Stem section, ventral side proximal to apical line (Al); notice the 'diagenetic' zone (d, 'type-A'). × 76.

Figs. 2–5. *Cylindroteuthis puzosiana* (d'Orbigny), Callovian, England. 2, sector no. 1 showing orientated crystals; 5% acetic acid, 30 mins. × 378·4. 3, sector no. 2 showing different extinction from sector no. 1, and crystals are orientated in a different direction; 5% acetic acid, 30 mins. × 378·4. 4, stem section; gun voltage, 10 kV; half of slab treated with 1% HCl for 6 mins., other side protected by tape; then the HCl-side (HCl) was protected and the other side treated with 25% glutardialdehyde (pH ~ 4) for 20 mins. (Glu); in the HCl-zone, the topographic high layers (TH) contain the most organic matter. × 79. 5, detail of fig. 4 showing HCl and mixed zones (Mi). In the mixed zone the glutaric acid component can be seen to 'work best' where there is an abrupt change in topography; i.e. change in content of organic matter (fat arrows). × 400.

Figs. 6–8. *Neohibolites minimus* (Miller), Middle Albian, England. 6, close-up of fractured specimen; no etching; note laminar habit of fracture. × 2190. 7, perpendicular view of surface; no etching; notice radial structures (r) are easily seen even in unetched specimens; s, inter-radial porous zones. × 500. 8, oblique view of surface (su) and radial structures of cross-section; 1% HCl, 1 min.; gun voltage 20 kV; note that radial structures (r) are composed of smaller units; g, growth-rings. × 200.

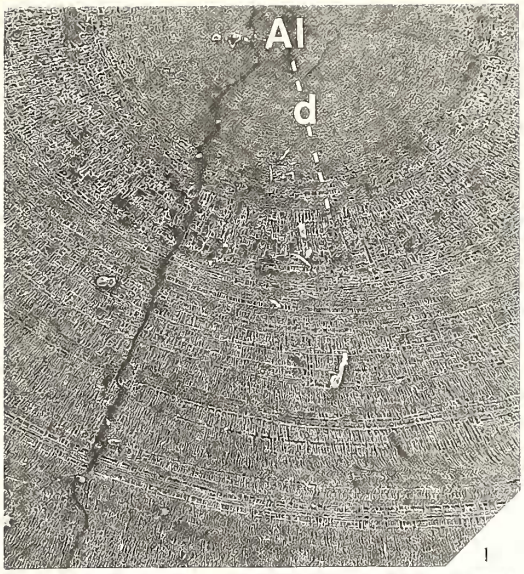

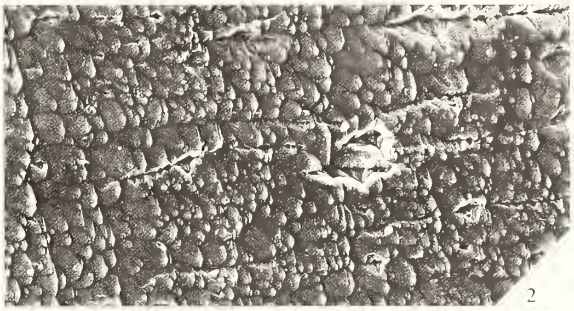

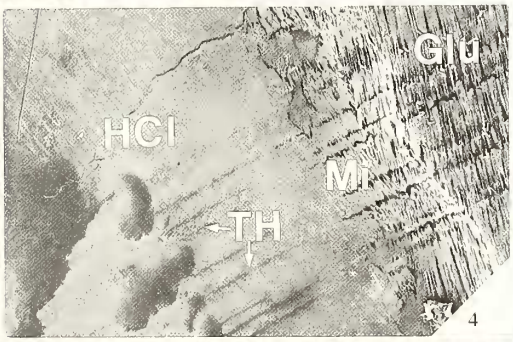

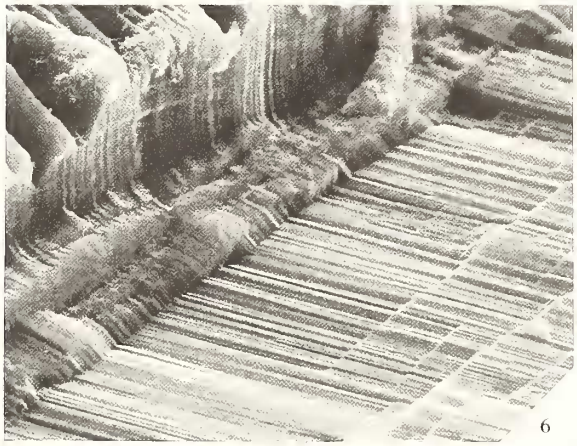

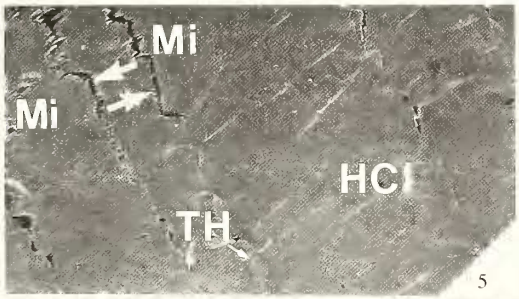

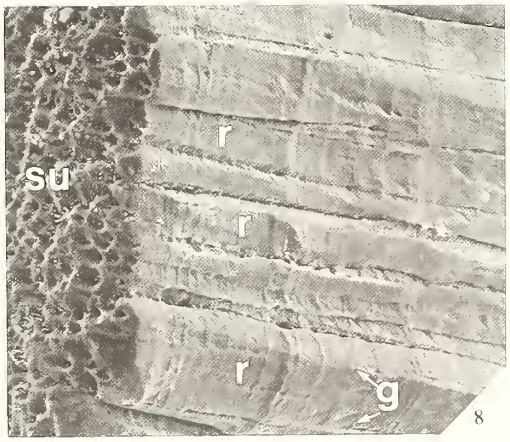

SÆLEN, *Belemnellocamax*, *Cylindroleuthis*, *Neohibolites*

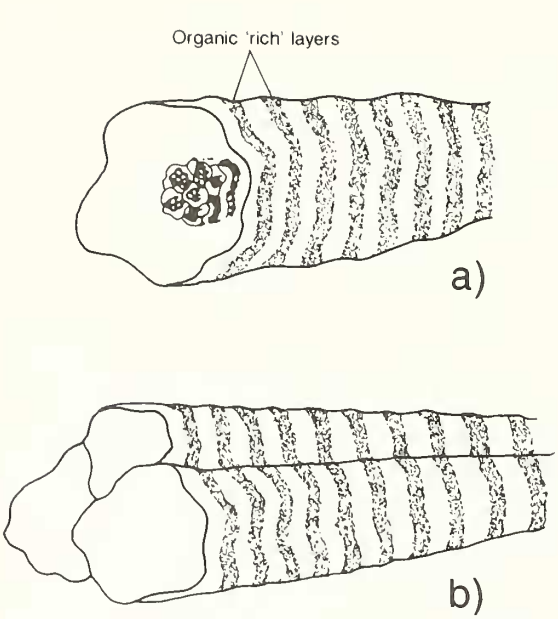

TEXT-FIG. 15. Laminated radial structures; a, radial structure composed of smaller units; b, a bundle of radial structures.

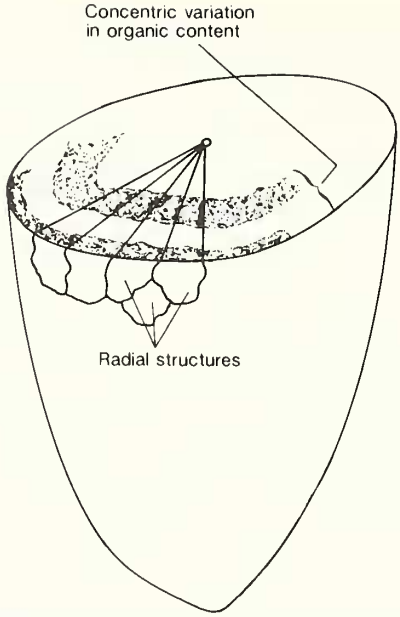

TEXT-FIG. 16. Schematic figure showing proposed construction of the belemnite rostrum.

nicols, can be ascribed to an irregular shape and stacking or radial structures (see text-fig. 17; Pl. 84, fig. 2; Pl. 87, fig. 8). This interpretation is supported by examinations under SEM (text-fig. 18 and Pl. 87, figs. 2 and 3). Most authors so far have proposed a diagenetic explanation for these structures (e.g. Müller-Stoll 1936, p. 177; Barskov 1970; Spaeth 1971*a*, p. 22). However, Recent Mollusca frequently show a similar image with bundles of radiating and indented crystals 'transected' by growth lines (Wilbur 1972, p. 125, and Grégoire 1972, pp. 47–51). It is thus feasible that this may be an original feature of belemnite rostra as well.

The original porosity of the rostra is as yet unknown. The data presented in this study do not indicate a high porosity, but in periods when low-Mg calcite was a stable mineral phase in sea water (Wilkinson 1982), an early marine cementation would make the original porosity difficult to recognize.

Comparison with Sepia *sp.*

Some authors (Spaeth 1971*a*, p. 35, 1973, p. 168; Spaeth *et al.* 1971, p. 3148, see also Barskov 1972, p. 497) have pointed out the resemblance between the internal structure of the porous *Sepia* cuttlebone and that of the rostral fabrics of belemnites (see Pl. 86, fig. 5). As can be seen from SEM micrographs, *Sepia* cuttlebones consist of septa connected by transverse 'palisades' made up of smaller units. The palisades are, again, made up of laminar elements (text-fig. 19). As already pointed out, a laminar construction of radial structures is also characteristic of belemnite rostra (Pl. 87, figs. 6 and 8). This apparent resemblance in morphology, however, does not necessarily indicate a close genetic similarity between *Sepia* and belemnites (Spaeth 1975, p. 329); the chambered cuttlebone permits buoyancy regulation through liquid and gas adjustments (Denton and Gilpin-Brown 1961; Denton 1974), whereas belemnites most probably made these adjustments through a homologous feature – the phragmocone (Stevens 1965; Spaeth 1975). Nevertheless, some authors (Veizer 1974; Spaeth 1975) have postulated an original porosity of 10–20% for belemnite rostra, which does not preclude the possibility that it was involved in buoyancy regulation in a similar way to the cuttlebone (Spaeth 1975, p. 329). However, in contrast to *Sepia* sp., the porosity of specimens

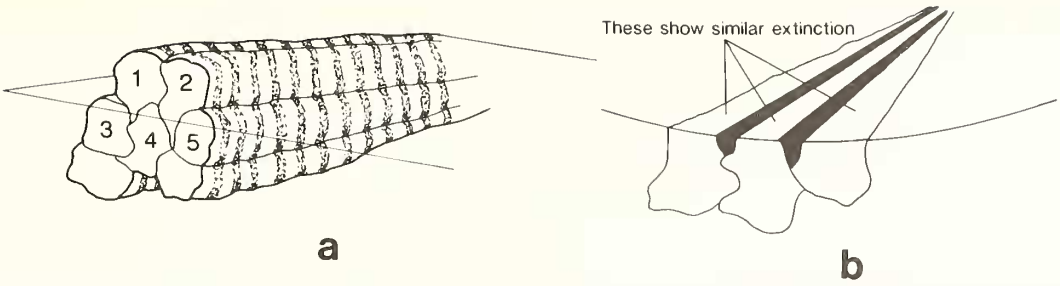

TEXT-FIG. 17 *a*, section through a bundle of radial structures; there is a slightly different crystal orientation in 1, 2 compared to 3, 4 and 5; *b*, thin-section through the plane shown in A.

TEXT-FIG. 18. Delimitation of two sectors by means of a silver colloidal paint to make them visible under SEM. Etching of these two sectors revealed crystals of different orientation (see also Pl. 87, figs. 2 and 3).

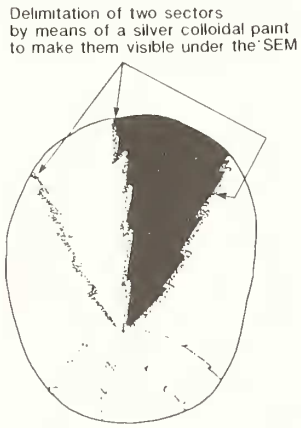

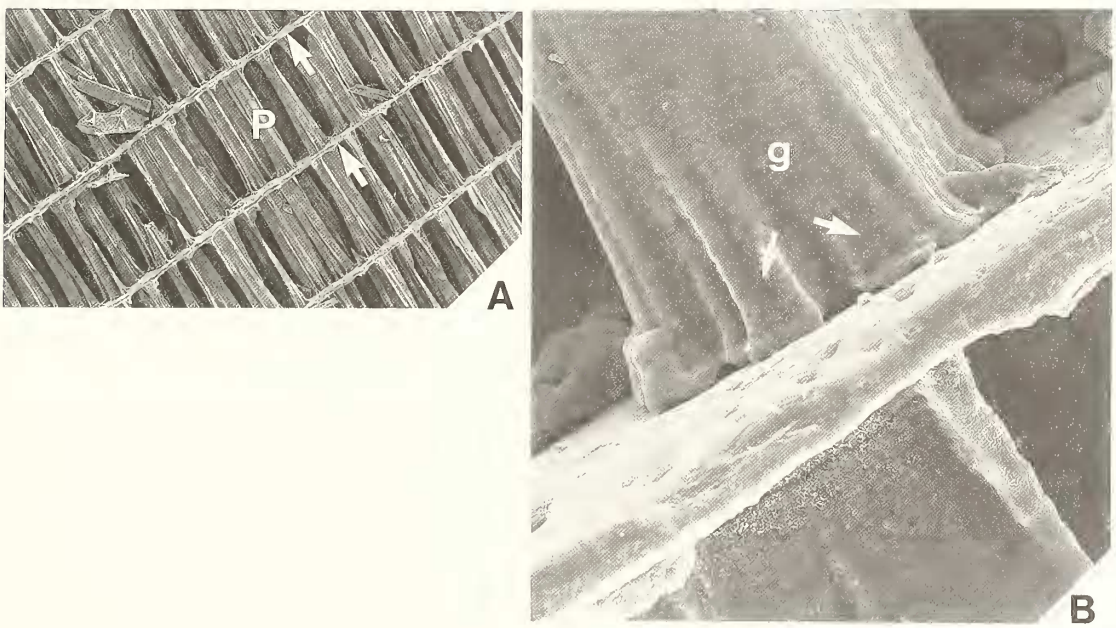

TEXT-FIG. 19. *Sepia* sp., Recent, Atherfield Point, Isle of Wight, Grid. ref. SZ 452790; no etching; A, palisades (P) and septa (arrows) of cuttlebone, ×34·4; B, close-up of palisade and septum in (A), notice composite structure (arrows) of each radial element (i.e. palisade), and their laminar construction (g). ×688.

in the present study was probably too low to have maintained such a mechanism (the maximum distance between radial structures for one *N. minimus* examined was 1 μm, whereas the distance between palisades in a cuttlebone is around 100 μm). A factor that complicates such a comparison is the partial modification of belemnite rostra. It would, however, seem odd that two morphologically different parts of the shell (the phragmocone and the rostrum) should regulate buoyancy through the same mechanism. A buoyancy-regulating function might nevertheless be expected for the rostrum, but merely as a counterweight (Stevens 1965, p. 49; Denton 1974, p. 292).

CONCLUSIONS

1. The experiments with etching, oxidizing and fixing agents on cross-sections of belemnite rostra revealed, under SEM, a common basic morphology of presumably original laminae in all species.

2. The original mineralogy was low-Mg calcite, and the present data indicate that the principal diagenetic changes involved.

A. Dissolution of intercrystalline organic material and precipitation of early cement (possibly high-Mg calcite, later transformed into low-Mg calcite), and with subsequent recrystallization of the carbonate portion of organic-rich laminae; these are bright luminescent and fluorescent ('type-A'), and recognizable under SEM.

B. Partial recrystallization, revealed by the faintly reddish CL-pattern ('type-C'). One cannot, however, exclude the possibility that rims of syntaxial cement are present, nor that diagenesis is partly expressed as a differential change in elemental composition.

C. Fracturing of the rostrum with precipitation of ferroan cement in fractures and dissolved laminae ('type-B' luminescence).

Diagenesis did not affect the rostra studied in such a way as to destroy the specific laminar morphology beyond recognition, and the present data indicate further that the rostrum was rather impervious.

3. SEM, CL and BLF data, make the author conclude that the interpretation proposed by Müller-Stoll (1936, p. 176), of a rostrum composed of alternating discrete 'organic' and 'inorganic' layers, is invalid. The original rostrum more probably consisted of radial structures that accreted periodically in a concentric fashion. The concentric 'non-diagenetic' pattern observed is thus due to a laminar variation in the organic content, which was probably both inter- and intra-crystalline. The variation in organic content is often subtle, so that growth-layers may be difficult to define.

Acknowledgements. I thank Prof. Dr M. R. Talbot and Dr W. Nemec (Bergen University) for critical reading of the manuscript; Å. Scheie (Norsk Hydro Research Centre, Bergen) for invaluable help regarding the SEM technique; Dr W. K. Christensen (Geological Museum of Copenhagen) for providing me with 40 specimens of *B. mammillatus* s.s.; Dr H. Powell (Oxford University Museum) for providing me with 19 specimens of *C. puzosiana*; O. Walderhaug (Rogalandsforskning), for providing me with the specimens of *A. speetonensis* and *N. ewaldi*; G. Torkildsen (Norsk Hydro Research Centre, Bergen) and H. Wraamann, H. Stenseth and B. Stavenes (Bergen University), for preparation of thin-sections; T. Rolfsen (Bergen University) and J. Rykkje (Norsk Hydro Research Centre, Bergen), for assisting me with SEM; C. Aakvaag and J. B. Olsen (Norsk Hydro Research Centre, Bergen) for running the TOC analyses; E. Irgens and J. K. Ellingsen (Bergen University), for skilled drafting.

REFERENCES

AL-AASM, I. S. and VEIZER, J. 1986. Diagenetic stabilization of aragonite and low-Mg calcite, 1. Trace elements in rudists. *J. sedim. Petrol.* **56,** 138–152.

BANDEL, K., ENGESER, T. and REITNER, J. 1984. Die Embryonal Entwicklung von *Hibolithes* (Belemnitida, Cephalopoda). *Neues Jb. Geol. Paläont. Abh.* **167,** 275–303.

BARSKOV, I. S. 1970. Structure of the belemnitid rostrum *Paleont. J.* **4,** 110–112.

—— 1972. Microstructure of the skeletal layers of belemnites compared with external shell layers of other mollusks. *Paleont. J.* **4,** 492–500.

BATHURST, R. G. C. 1975. *Carbonate sediments and their diagenesis*, 658 pp. Amsterdam, Elsevier.

BAYER, U. 1975. Organische Tapeten im Ammoniten-Phragmokon und ihr Einfluss auf die Fossilisation. *Neues Jb. Geol. Paläont. Mh.* **1,** 12–25.

BAYLE, E. 1878. *Explication de la carte géologique de France Tome quatrième. Première. Fossiles principaux des Terrains.* Atlas. – (Imprimerie Nationale) Paris.

BERNER, R. A. 1980. *Diagenesis – a theoretical approach*, 241 pp. Princeton University Press, Princeton.

BRAND, U. and MORRISON, J. O. 1987. Biogeochemistry of fossil marine invertebrates. *Geoscience Can.* **14,** 85–106.

CASEY, R. 1966. Palaeontology of the Gault, 102–113. *In* SMART, J. G. O., BISSON, G. and WORSSAM, B. C. (eds.). Geology of the country around Canterbury and Folkestone. *Mem. Geol. Surv. U.K.*

CHAVE, K. E. 1952. A solid solution between calcite and dolomite. *J. Geol.* **60,** 190–192.

CHRISTENSEN, W. K. 1975. Upper Cretaceous belemnites from the Kristianstad area in Scania. *Fossils Strata*, **7,** 69 pp.

CURTIS, C. D. 1980. Diagenetic alteration in black shales. *J. geol. Soc. Lond.* **137,** 189–194.

—— 1987. Mineralogical consequences of organic matter degradation in sediments: Inorganic/organic diagenesis, pp. 108–123. *In* LEGGETT, J. K. and ZUFFA, G. G. (eds.) *Marine Clastic Sedimentology*.

CZERNIAKOWSKI, L. A., LOHMANN, K. C. and WILSON, J. L. 1984. Closed system marine diagenesis: isotopic data from the Austin Chalk and its components. *Sedimentology*, **31,** 863–877.

DENTON, E. J. 1974. On the buoyancy and the lives of modern and fossil cephalopods. *Proc. R. Soc. Lond.* **B 185,** 273–299.

DENTON, E. J. and GILPIN-BROWN, J. B. 1961. The buoyancy of the cuttlefish *Sepia officinalis* (L). *J. mar. biol. Ass. U.K.* **41,** 319–342.

DICKSON, J. A. D. 1966. Carbonate identification and genesis as revealed by staining. *J. sedim. Petrol.* **36,** 491–505.

DRAVIS, J. B. and YUREWICZ, D. A. 1985. Enhanced carbonate petrography using fluorescence microscopy. *J. sedim. Petrol.* **55,** 795–804.

DROZDOVA, T. V. 1969. Organic matter in belemnites. *Geokhimya*, **10,** 1281–5. [In Russian.]

DUFF, K. L. 1975. Palaeoecology of a bituminous shale – the lower Oxford Clay of central England. *Paleontology*, **18,** 443–482.

FAIRCHILD, I. J. 1983. Chemical controls of cathodoluminescence of natural dolomites and calcites: new data and review. *Sedimentology*, **30,** 579–583.

FRANK, J. R., CARPENTER, A. B. and OGLESBY, T. W. 1982. Cathodoluminescence and composition of calcite cement in the Taum Sauk Limestone (Upper Cambrian), Southeast Missouri. *J. sedim. Petrol.* **52,** 631–638.

FRITZ, P. 1965. O^{18}/O^{16}-Isotopenanalysen und Paleotemperaturbestimmungen an Belemniten aus den Schwäbischen Jura. *Geol. Rdsch.* **54,** 261–269.

GIJZEL VAN, P. 1979. Manual of the techniques and some geological applications of fluorescence microscopy. *American Association of Stratigraphic Palynologists.* 12th Annual Meeting Dallas oct. 29–nov. 2.

GLOVER, E. D. 1977. *Cathodoluminescence, iron and manganese content and the early diagenesis of carbonates.* 444 pp., Ph.D. Dissertation, University of Wisconsin-Madison.

GREGOIRE, C. 1972. Structure of the Molluscan Shell, 45–102. *In* FLORKIN, M. and SCHEER, B. T. (eds.). *Chemical Zoology VII. Mollusca.* Acadamic Press New York and London.

HALL, A. and KENNEDY, W. J. 1967. Arogonite in fossils. *Proc. R. Soc. Lond.* **B 168,** 377–412.

HAVE, ten T. and HEIJNEN, W. 1985. Cathodoluminescence activation and zonation in carbonate rocks: an experimental approach. *Geol. Mijnb.* **64,** 297–310.

HUDSON, J. D. 1978. Concretions, isotopes, and the diagenetic history of the Oxford Clay (Jurassic) of Central England. *Sedimentology*, **25,** 339–370.

HÜKEL, U. and HEMLEBEN, CH. 1976. Diagenetische Spurelement-Verschiebungen und Veränderungen der Skelett-Strukturen bei Belemniten-Rostren. *Zentbl. Geol. Paläont.* Teil II, 362–365.

IVERSEN, T. H. 1973. *Elektronmikroskopi.* 108 pp. Tapir.

JELETZKY, J. A. 1965. Taxonomy and phylogeny of fossil Coleoidea (= Dibranchiata). *Geol. Surv. Pap. Can.*, **65,** No. 42, 72–76.

—— 1966. Comparative morphology, phylogeny, and classification of fossil Coleoidea. Mollusca, *Paleont. Contr. Univ. Kans.* article 7, 162 pp.

KÜSPERT, W. 1982. Environmental changes during oil shale deposition as deduced from stable isotope ratios, 482–501. *In* EINSELE, G. and SEILACHER, A. (eds.). *Cyclic and event stratification.*

LONGINELLI, A. 1969. Oxygen-18 variations in belemnite guards. *Earth Planet. Sci. Lett.* **7,** 209–212.

LUTZ, R. A. and RHOADS, D. C. 1980. Growth pattern within the molluscan shell, 203–254. *In* RHOADS, D. C. and LUTZ, R. A. (eds.). *Skeletal growth of aquatic organisms: biological records of environmental change.* Plenum Press, New York and London.

MACHEL, H-G. 1985. Cathodoluminescence in calcite and dolomite and its chemical interpretation. *Geoscience Can.* **12,** 139–147.

MASON, R. A. 1987. Ion microprobe analysis of trace elements in calcite with an application to the

cathodoluminescence zonation of limestone cements from the Lower Carboniferous of South Wales, U.K. *Chem. Geol.* **64**, 209–224.

MILLER, J. S. 1826. Observations on Belemnites V. *Trans. geol. Soc. Lond. 2 Ser.* **1**, 45–62.

MONTFORT, D. de 1808. *Conchyologie systématique et classification méthodique des coquilles.* (Schoell) Paris.

MUTTERLOSE, J. 1983. Phylogenie und Biostratigraphie der Unterfamilie (Belemnitida) aus dem Barrême (Unter-Kreide) NW-Europas. *Palaeontographica* **A 180**, 1–90.

MÜLLER-STOLL, H. 1936. Beiträge zur Anatomie der Belemnoidea. *Nova Acta Leopoldina*, new series **4**, 159–226. Halle (Saale).

NAEF, A. 1922. *Die fossilen Tintenfische*, 322 pp. S., Jena G. Fischer.

NAIDIN, D. P. 1964. The Upper Cretaceous belemnites of the Russian Platform and contiguous regions, *Actinocamax*, *Gonioteuthis*, *Belemnellocamax*, 190 pp. Moscow University Press. [In Russian.]

NEALE, J. W. 1974. Chap. 8: Cretaceous, 225–243. *In* RAYNER, D. A. and HEMINGWAY, J. E. (eds.). *The Geology and mineral resources of Yorkshire.* Yorkshire Geol. Soc.

NICKEL, E. 1978. The present status of cathodoluminescence as a tool in sedimentology. *Miner. Sci. Eng. (Johannesb.)* **10**, 73–100.

NILSSON, S. 1826. Om de mångrummiga snäckor som förekomma i Kritformationen i Sverige. *K. Svenska Vetensk.-Akad. Handl.* (1825), 329–343.

OLDERSHAW, A. E. and SCOFFIN, T. P. 1967. The source of ferroan and non-ferroan calcite cements in the Halkin and Wenlock Limestones. *J. Geol.* **5**, 309–326.

D'ORBIGNY, A. 1845. *Paléontologie universelle des coquilles et des mollusques.* (Masson) Paris.

—— 1847. *Paléontologie française. Terrains Cretacés. Supplement*, 28 pp. Paris.

—— 1860. *Paléontologie française. Terrains jurassiques. Paris.*

OWEN, H. G. 1972. The Gault and its junction with the Woburn Sands in the Leighton Buzzard Area, Bedfordshire and Buckinghamshire. *Proc. Geol. Ass.* **83**, 287–312.

PAVLOV, A. P. 1982. Belemnites du Speeton, 455–570. *In* PAVLOV, A. P. and LAMPLUGH, G. (eds.). Argilles du Speeton et leurs equivalents. *Bull. Soc. Nat. Moscou*, N. Ser. **3.**

—— 1914. Yurskie i nizhnemelovye Cephalopoda severnot Sibiri. *Zap. Imp. Akad. Nauk, ser. 8, Fiz.-mat. Otd.* **21**, (4), 68 pp. [in Russian.]

PHILLIPS, J. 1865. A monograph of British Belemnitidae. *Paleontogr. Soc.* [*Monogr.*], 130 pp.

PIERSON, B. J. 1981. The control of cathodoluminescence in dolomite by iron and manganese. *Sedimentology*, **28**, 601–610.

POPP, B. N., ANDERSON, T. F. and SANDBERG, P. A. 1986. Textural, elemental, and isotopic variations among constituents in Middle Devonian Limestones, North America. *J. sedim. Petrol.* **56**, 715–727.

RAGLAND, P. C., PILKEY, O. H. and BLACKWELDER, B. J. 1979. Diagenetic changes in the elemental composition of unrecrystallized Mollusk shells. *Chem. Geol.* **25**, 123–134.

RAWSON, P. F. 1972. A note on the biostratigraphical significance of the lower Cretaceous belemnite genus *Aulacoteuthis* in the B-beds of the Speeton Clay, Yorkshire. *Proc. Yorks. geol. Soc.* **39**, 89–91.

ROGÉR, J. 1952. Sous-classe des Dibranchiata Owen, 1836, *In* PIVETEAU, J. (ed.): *Traité de paléontologie* **2**, 689–755. Masson, Paris.

RICHTER, D. K. and FÜCHTBAUER, H. 1978. Ferroan calcite replacement indicates former magnesian calcite skeletons. *Sedimentology*, **25**, 843–860.

RIEGRAF, W. 1981. Revision der Belemniten des Schwäbischen Jura. *Palaeontographica* **A 173**, 64—139.

SABATINI, D. D., MILLER, F. and BARRNETT, R. J. 1964. Aldehyde fixation for morphological and enzyme histochemical studies with the electron microscope. *J. Histochem. Cytochem.* **12**, 57.

SÆLEN, G. and KARSTANG, T. V. 1989. Chemical signatures of belemnites. *N. Jb. Geol. Paläont. Abh.* **177**, 333–346.

SANDBERG, P. A. 1983. Recognition criteria for calcitized skeletal and non-skeletal aragonites. *Palaeontogr. am.* **54**, 272–281.

—— 1985. Nonskeletal aragonite and pCO_2 in the Phanerozoic and Proterozoic. *In* SUNDQUIST, E. T. and BROECKER, W. S. (eds.). The carbon cycle and atmospheric CO_2: Natural variations Archean to Present. *Geophys. Monogr.* **32**, 585–594.

SPAETH, C. 1971*a*. Untersuchungen an Belemniten des Formenkreises um *Neohibolites minimus* (Miller 1826) aus dem Mittel – und Ober-Alb Nordwestdeutschlands. *Geol. Jb.* **100**, 127 pp.

—— 1971*b*. Aragonitische und calcitische Primär-strukturen im Schalenbau eines Belemniten aus der englischen Unterkreide. *Paläont. Z.* **45**, 33–40.

—— 1973. Weitere Untersuchungen der Primär- und Fremdstrukturen in calcitischen und aragonitischen Schalenlagen englischer Unterkreide-Belemniten. *Paläont. Z.* **47**, 163–174.

SPAETH, E. 1975. Zur Frage der Schwimmverhältnisse bei Belemniten in Abhängigkeit vom Primärgefüge der Hartteile. *Paläont. Z.* **49,** 321–331.

——, HOEFS, J. and VETTER, U. 1971. Some aspects of isotopic composition of belemnites and related 'paleotemperatures'. *Bull. geol. Soc. Am.* **82,** 3139–3150.

STEVENS, G. R. 1965. The Jurassic and Cretaceous belemnites of New Zealand and a review of the Jurassic and Cretaceous belemnites of the Indo-Pacific region. *Bull. geol. Surv. N.Z.* **36,** 233 pp.

STEVENS, G. R. and CLAYTON, R. N. 1971. Oxygen isotope studies on Jurassic and Cretaceous belemnites from New Zealand and their biogeographic significance. *N.Z. Jl Geol. Geophys.* **14,** 829–887.

STOLLEY, E. 1911. Studien an den Belemniten der unteren Kreide Norddeutschlands. *Jber. niedersächs. geol. Ver.* **4,** 174–191.

—— 1919. Die Systematik der Belemniten. *Jber. niedersächs. geol. Ver.* **11,** 1–70.

STROMBECK, A. von 1861. Über den Gault und insbesondere die Gargas-Mergel im nordwestlichen Deutschland. *Z. dt. geol. Ges.* **13,** 20–60.

STURZ-KÖWING, I. 1960. Veränderungen im Inneren von Belemnitenrostren des oberen Lias. *Shr. naturw. Ver. Schlesw.-Holst.* **30,** 60–67.

SWINNERTON, H. H. 1936–55. A monograph of British Cretaceous Belemnites. *Palaeontogr. Soc.* [*Monogr.*], 86 pp.

TAN, F. C. and HUDSON, J. D. 1974. Isotopic studies on the palaeoecology and diagenesis of the Great Estuarine Series (Jurassic) of Scotland. *Scott. J. Geol.* **10,** 91–128.

UREY, H. C., LOWENSTAM, H. A., EPSTEIN, S. and MCKINNEY, G. R. 1951. Measurement of paleotemperatures and temperatures of the Upper Cretaceous of England, Denmark, and the Southeastern United States. *Bull. geol. Soc. Am.* **62,** 399–416.

VEIZER, J. 1974. Chemical diagenesis of belemnite shells and possible consequences for paleotemperature determination. *Neues Jb. Geol. Paläont. Abh.* **147,** 91–111.

—— 1983. Chemical diagenesis of carbonates, Chapter 3: Theory and application of trace element technique, 3–1 – 3–100. *In* ARTHUR A. (ed.). *Stable isotopes in sedimentary geology*. SEPM short course No. 10, Dallas.

VETTER, U. 1968. Röntgenographische Gefügeuntersuchungen am Calcit einiger Belemnitenrostren. *Neues Jb. Miner. Abh.* **109,** 274–288.

WESTBROEK, P., VAN DER MEIDE, P. H., VAN DER WEY-KLOPPERS, J. S., VAN DER SLUIS, R. J., DE LEEUW, J. W. and DE JONG, E. W. 1979. Fossil macromolecules from cephalopod shells: characterization, immunological response and diagenesis. *Paleobiology*, **5,** 151–167.

WILBUR, K. M. 1972. Shell formation in mollusks, 103–145. *In* FLORKIN, M. and SCHEER, B. T. (eds.). *Chemical Zoology VII. Mollusca*. Academic Press, New York and London.

WILKINSON, B. H. 1982. Cyclic cratonic carbonates and Phanerozoic calcite seas. *J. geol. Education*. **30,** 189–203.

WILSON, V. 1948: East Yorkshire and Lincolnshire. 94 pp. *Geological Survey and Museum, London.*

ZITTEL, K. A. 1895. *Grundzüge der Paläontologie*. Oldenbourg, München und Leipzig.

GUNNAR SÆLEN,
Geologisk Institut Avd. A,
Universitetet I Bergen,
Allégt. 41, N-5007 Bergen,
Norway

Typescript received 27 April, 1988
Revised typescript 23 January, 1989